CHAPTER FIVE

MTO Processes Development: The Key of Mesoscale Studies

Mao Ye[1], Hua Li, Yinfeng Zhao, Tao Zhang, Zhongmin Liu

Dalian National Laboratory for Clean Energy and National Engineering Laboratory for MTO, Dalian Institute of Chemical Physics, Chinese Academy of Sciences, Dalian, PR China

[1]Corresponding author: e-mail address: maoye@dicp.ac.cn

Contents

Advances in Chemical Engineering, Volume 47
ISSN 0065-2377
http://dx.doi.org/10.1016/bs.ache.2015.10.008

Abstract

Methanol to olefins (MTO), which provides a new route to produce light olefins such as ethylene and propylene from abundant natural materials (e.g., coal, natural gas or biomass), has been recently industrialized by the Dalian Institute of Chemical Physics (DICP), Chinese Academy of Sciences. In this contribution, the process development of MTO is introduced, which emphasizes the importance of mesoscale studies and focuses on three aspects: a mesoscale modeling approach for MTO catalyst pellet, coke formation and control in MTO reactor, and scaling up of the microscale-MTO fluidized bed reactor to pilot-scale fluidized bed reactor. The challenges and future directions in MTO process development are also briefed.

1. INTRODUCTION

Light olefins such as ethylene and propylene are key components in the chemical industries. They are conventionally produced from petrochemical feedstock via naphtha thermal cracking and fluid catalytic cracking (FCC) processes (Corma, 2003; Primo and Garcia, 2014; Van Santen et al., 1999). The efforts to viable routes for producing light olefins from alternative resources other than oil have been continuously growing since the oil crisis in 1970s (Chang, 1984; Chang and Silvestri, 1977; Liang et al., 1990). Methanol, which can be readily produced from coal, natural gas, and biomass via synthesis gas ($CO + H_2$) by existing and proven technologies, offers an attractive choice (Chang, 1984; Chang and Silvestri, 1977; Keil, 1999; Tian et al., 2015). Early researches by scientists in Mobil discovered that a zeolite-based process could be used to convert methanol into gasoline. In this methanol to gasoline (MTG) process, a new class of synthetic shape-selective zeolites, namely ZSM-5, was used. Later on, Union Carbide reported the successful synthesis of a silicoaluminophosphate (SAPO) catalyst in 1980s. Scientists from the Dalian Institute of Chemical Physics (DICP), Chinese Academy of Sciences found that SAPO-34 catalyst could be used to convert the methanol to light olefins with high selectivity (Liang et al., 1990). Since then, methanol to olefins (MTO) process has become a subject of intense researches spanning catalyst synthesis, reaction mechanism, reaction kinetics, process development, and reactor scale-up. In August 2010, a commercial unit (600 kt/a of ethylene and propylene production) based on the DICP MTO process (DMTO) was successfully brought into stream in Shenhua's Baotou coal-to-olefins plant in north China (Liu et al., 2014). This is the world's first MTO commercial plant,

and its success represents an important milestone and breakthrough of MTO process development. So far, several MTO processes have been commercialized, which include, in addition to the DMTO process, the MTO process by UOP (Zhang, 2013), the methanol to propylene (MTP) process by Lurgi (Nan et al., 2014), and the SINOPEC's MTO (SMTO) process by SINOPEC (Jiang et al., 2014).

The catalysts synthesis, reaction mechanism and kinetics, process development, and reactor design and operation for industrial MTO processes require the detailed researches from molecular to reactor level due to the multiphase and multiscale nature, which cover a considerably broad range of space and time scales. From practical point of view, the understanding of the MTO reaction mechanism and shape selectivity to target products (ethylene and propylene) over relevant zeolite catalyst, which is the basis of reactor selection, process optimization, and unit operation for MTO process development, is of critical importance. In the past decades, a huge amount of work has been published studying the MTO process at different space and time scales. At very fundamental scale, modeling approaches such as quantum mechanics (QM) and molecular dynamics (MD) (Van Speybroeck et al., 2014), as well as high temporal and spatial resolution measurement techniques such as high-energy Operando X-ray diffraction (HXRD) and nuclear magnetic resonance (NMR) (Buurmans and Weckhuysen, 2012; Hunger et al., 2001; Li et al., 2015b; Wragg et al., 2012) were used to study the MTO reaction mechanism. At reactor level, macroscale experiments under either cold flow or reaction conditions, as well as computational fluid dynamics study were carried out to derive the gross reaction kinetics and monitor the fluid flow. Except that in a few cases, the macroscale reaction data have been used to deduce the reaction network, it is generally difficult to get the information of element steps, and thus, reaction mechanism in the zeolites with sufficient accuracy based on the macroscale reaction data. Meanwhile, the mechanistic researches, although being applied to instruct the MTO reaction controlling, the quantitative translation of the knowledge obtained from the fundamental scale to macroscale remains a hard task. The systematic theories and methods linked the fundamental scale to macroscale are yet to be developed. Therefore, the MTO process development, at current stage, is still dependent on the experience built via experiments at different scales. Li et al. (2013) classified the methods to bridge such gap as the mesoscale methods. Apparently, the studies at mesoscales play an important part in establishing the theories or methods for reaction-transport process linking two adjunct scales.

In this contribution, the development of MTO processes will be introduced. We will emphasize the mesoscale challenges and the related studies in the DMTO process development, for which we focus on three aspects: a mesoscale modeling approach for MTO catalyst pellet, the coke formation and control in MTO reactor, and the scale-up of the microscale-MTO fluidized bed reactor to pilot-scale. A section followed is dedicated to the future directions in MTO process development in terms of mesoscale studies.

2. MTO PROCESS DEVELOPMENT

Methanol is an important C_1 compound, and is very active over a variety of acidic zeolites with different topologies (pores, channels, and cavities), compositions (acid sites), and morphologies (crystal size, micro-, and mesopores) to form different hydrocarbons (Olsbye et al., 2012). As discussed above, ZSM-5 and SAPO-34 are two zeolites of industrial interests in converting methanol to light olefins. SAPO-34 has pore size of 0.38 nm, which shows high selectivity to ethylene and propylene (about 80%) but could be deactivated in several hours. Thus, a continuous regeneration is required for MTO process based on SAPO-34 catalyst. ZSM-5 has 10-membered ring openings with 3D pore structure, and the pore size is 0.54×0.57 nm. The larger pore size of ZSM-5 leads to a much wider product distribution. Heavy gasoline compounds are formed over ZSM-5 as by-product. In DMTO process developed by DICP, the SAPO-34 catalyst is used to convert methanol in fluidized bed reactor. In the following, the history of MTO process development is introduced.

2.1 MTG Processes

The successful synthesis of ZSM-5 zeolites which have relatively larger pore size and higher Si-to-Al ratio in early 1970s stimulates the rapid development of MTG process (Chang, 1983; Keil, 1999). Mobil first built a fixed bed pilot plant to demonstrate the feasibility of MTG process. In 1985, the MTG process was implemented into a commercial plant in New Zealand with a gasoline capacity of 14,500 bpd. Almost at the same time, Mobil also developed fluidized bed MTG technology, which was demonstrated in a 4 bpd pilot plant in Paulsboro, New Jeasey and scaled up to a demonstration scale of 100 bpd during 1981–1984 in Wesseling, Germany. This fluidized bed MTG demonstration unit stopped operation at the end of 1985 due to the lower price of oil at that time (Keil, 1999). Apparently, the

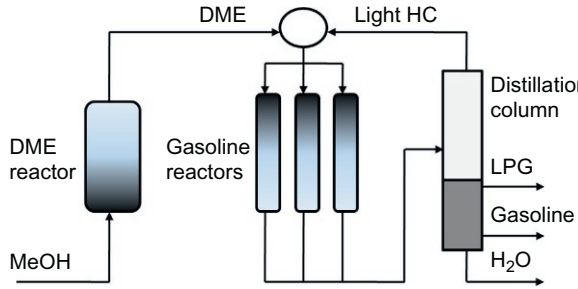

Figure 1 The schematic diagram of Mobil's MTG process.

early work by Mobil showed the confidence and feasibility of MTG process with ZSM-5 catalyst.

In Mobil's MTG process, the products spin from C_1 to C_{11} hydrocarbons, and among them the C_5^+ (benzene fraction) accounts to roughly 80%. Although ZSM-5 catalyst was shown feasible for MTG process, they would still deactivate slowly due to the deposition of coke. Therefore, several parallel reactors had been used in the MTG commercial unit in New Zealand, and the intermittent regeneration was used to maintain the continuous operation. Figure 1 shows the schematic diagram of Mobil's commercial MTG unit in New Zealand. In 1990s, ExxonMobil further optimized the MTG process and started to license the improved MTG process. In March 2010, the first MTG unit (100 kt/a gasoline product) in China was started up. This unit used the ExxonMobil MTG technology and was built in Jincheng, Shanxi. When oil price is low, the MTG process is economically less competitive.

2.2 DMTO Process

Light olefins are in fact intermediates in the MTG process. Careful controlling of the reaction conditions, e.g., temperature, pressure, and catalyst acidity can prompt the production of light olefins in the process of methanol conversion. Mobil's researchers demonstrated the MTO process based on ZSM-5 zeolites. In 1982, the scientists at DICP initiated a project on MTO research under the support by Chinese government and Chinese Academy of Sciences. A 300 t/a MTO-fixed bed pilot plant was constructed and operated in 1993 by DICP (Tian et al., 2015).

In 1986, Union Carbide reported the successful synthesis of a SAPO catalyst. Researchers from DICP found that SAPO-34 catalyst could be used to convert the methanol to light olefins with high selectivity (Liang et al., 1990). Except high selectivity to light olefins, SAPO-34 catalyst is readily

deactivated due to coke deposition. In this sense, fluidized bed is the best choice for MTO process based on SAPO-34 catalyst as deactivated catalyst can be regenerated online by circulating catalyst between reactor and regenerator. Note that the synthesis of dimethyl ether is thermodynamically more favorable than that of methanol, researchers from DICP first developed a syngas/dimethyl ether to olefins (SDTO) method in early 1990s. A pilot fluidized bed reactor for SDTO process was constructed and successfully tested in 1995. However, the SDTO process was economically less competitive when the oil price goes lower. To this end, the researchers from DICP focused on zeolite synthesis and modifications in order to further improve the catalyst performance (Tian et al., 2015). Great success was achieved by the DICP team in synthesizing high efficient and economic MTO fluidized bed catalyst (Tian et al., 2015).

Meanwhile, DICP team also tried to scale-up the MTO process in the laboratory. In 2004, they finished the MTO pilot-scale experiments and decided to build a MTO demonstration unit (16 kt/a Methanol feed) and scale-up the MTO process to commercial scale. Two partners, Shaanxi Xinxin Coal Chemical Ltd. and Luoyang Petrochemical Engineering Corporation, joined in DICP team to construct the demonstration unit, which was completed in July 2005. In December 2005, the MTO demonstration unit was brought on stream. In June 2006, DICP announced the success of the operation of MTO demonstration unit and started to license the MTO technology, which is now called DMTO technology. Based on DMTO technology, the world's first MTO commercial unit (600 kt/a of ethylene and propylene production) was started up in August 2010 in Shenhua's Baotou coal-to-olefins plant in north China (Liu et al., 2014). Figure 2 is the schematic diagram of Shenhua's DMTO unit.

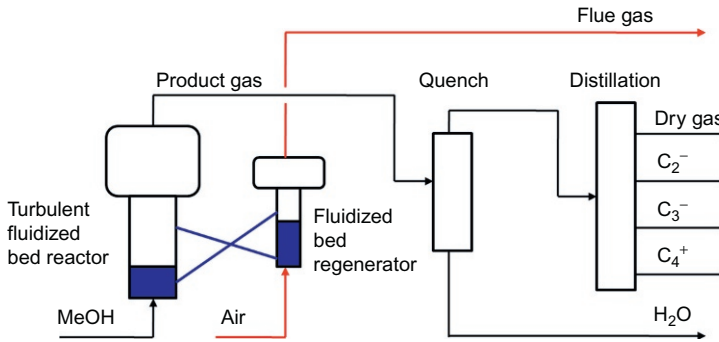

Figure 2 The schematic diagram of DMTO process.

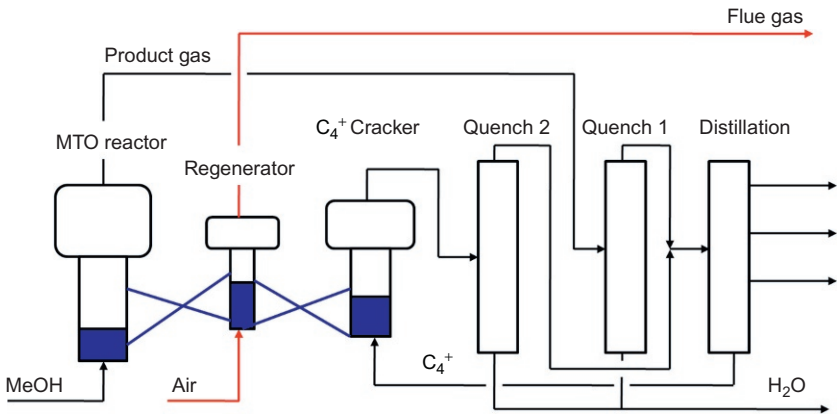

Figure 3 The schematic diagram of DMTO-II process.

In order to achieve a higher light olefins yield, DICP synthesize a new dual-functional catalyst, over which both the MTO reaction and C_4^+ hydrocarbon cracking reaction can be realized. Based on this catalyst, DICP developed the DMTO-II process. In the DMTO-II process, the C_4^+ compounds are recycled to the fluidized bed C_4^+ cracking reactor to increase the ethylene and propylene yield. As there is only one catalyst in this process, a single fluidized bed regenerator is possible. This can significantly simplify the process and improve the utility efficiency. In September 2009, DICP revamped the DMTO demonstration unit and upgraded it to a DMTO-II demonstration unit. In May 2010, the DICP announced that the experiments of DMTO-II process was successful and started to license the DMTO-II technology. At the end of 2014, the first DMTO-II unit (with 670 kt/a of ethylene and propylene production) was commissioned and started its commercial operation (the scheme of the DMTO-II process shown in Fig. 3). Until December 2014, there are six DMTO commercial units and one DMTO-II commercial unit in operation, with a total capacity of 417 kt/a of ethylene and propylene production.

2.3 MTO Process by UOP

UOP has long been working with the MTO catalyst and process development. In June 1995, UOP and Norsk Hydro (now INEOS) built a fluidized bed MTO pilot plant with a capacity of 0.75 t/d methanol feed. In this pilot plant, the reactor–regenerator and product separation system were included (Vora et al., 1997). To further improve the selectivity to ethylene and propylene, UOP combined the UOP/Hydro MTO process with TOTAL's

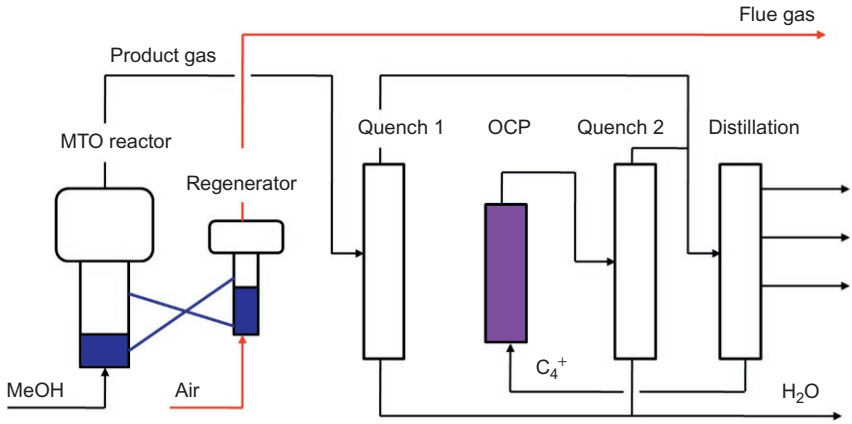

Figure 4 The schematic diagram of UOP's MTP/OCP process.

olefin cracking process (OCP), and the latter could crack the C_4^+ compounds into ethylene and propylene. Together with TOTAL, UOP constructed a demonstration unit in Feluy, Belgium, which, as schematically shown in Fig. 4, can process roughly 10 ton methanol feed per day. In 2009, this demonstration unit was started up. The combined MTO/OCP process has two separate reaction systems, i.e., a fluidized bed MTO system and a fixed bed C_4^+ cracking system. Compared to the DMTO-II process, two catalysts have to be used in UOP's MTO/OCP process. In 2013, the first commercial unit based on UOP's MTO process (the capacity is 295 kt/a of light olefins production) was commissioned in Nanjing, China (Zhang, 2013).

2.4 Other MTO Processes

Besides Mobil, DICP, and UOP, SINOPEC has been actively involved in the MTO process development since 2000 (Liu, 2015). In 2005, a pilot-scale MTO unit capable of processing 12 t/a methanol feed was built in Shanghai. The SMTO process follows that of DICP and UOP, in which SAPO-34 catalyst is used. The SMTO process (100 t/d of methanol feed) has been demonstrated in Yanshan in Beijing in 2007. In 2011, an industrial SMTO unit with a capacity of 200 kt/a ethylene and propylene was brought on stream in Henan, China (Jiang et al., 2014).

Lurgi follows the route as originally developed by Mobil, and the ZSM-5 zeolite catalyst is used to convert methanol. Unlike DICP and UOP, Lurgi particularly concentrates on the propylene yield, which leads to the

development of a fixed bed MTP process. In order to maximize the propylene yield, the by-products are recycled to the fixed bed reactor for further conversion. In 2011, the first fixed bed MTP commercial unit was commissioned in Ningxia in China. The unit reached its full capacity close to 500 kt/a of propylene 1 year later (Nan et al., 2014).

In parallel to the Lurgi fixed bed MTP process, Tsinghua University proposed a fluidized bed MTP (FMTP) process based on the SAPO-18/34 zeolite catalyst. It was declared that this catalyst can limit the formation of the compounds of C_4 and beyond, and thus prompt the yield of ethylene and propylene. FMTP process has two fluidized bed reactors. The first one is used to convert methanol to light olefins, and the second one is mainly for further converting ethylene and butylenes to propylene. In 2008, Tsinghua, together with its partners, built a FMTP demonstration unit (capacity of 30 kt/a of methanol feed) in Anhui, China. In September 2009, the demonstration unit was started up. The experimental data shows that the methanol conversion is almost 100%, and the propylene yield is close to 67.3% (CH_2 basis). FMTP has not been industrialized so far.

3. MULTISCALE NATURE OF MTO PROCESS

Apparently, the development of MTO process has an inherent multiscale nature, as shown in Fig. 5. The optimal design of an industrial MTO fluidized bed reactor requires the detailed information from molecular to reactor scales, which covers the space scale of nm to m by an order of 9 to 10.

3.1 Reaction Mechanism at Molecular Scale

At molecular scale (~nm), the conversion of methanol molecules to either intermediates or final products over zeolite needs to be understood. Great efforts have been devoted to study the formation of initial C—C bonds as methanol is a typical C_1 compound. More than 20 possible mechanisms were proposed by various groups, and most of them, however, lack of direct experimental evidences. Song et al. (2002) and recently Qi et al. (2015) proposed that the impurities of feedstock from different sources might be the reason for the initial C—C bonds formation. Nevertheless, the consent

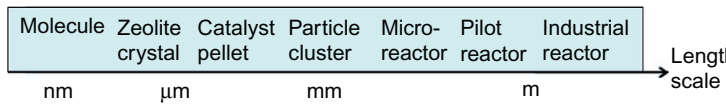

Figure 5 The multiscale nature of MTO process development.

on the mechanism of the initial C—C bonds formation is far from being reached. Of practical importance is the reaction path in MTO process. Hydrocarbon pool proposed by Dahl and Kolboe (1994) is now widely accepted as the main path for MTO reaction. The hydrocarbon pool refers to organic species, $(CH_2)_n$, confined in the zeolite cage or intersection of channels, which can further assemble olefins from methanol feed. Many researches concentrated on the mechanism underlying the hydrocarbon pool formation, the intermediate species, and the element steps in MTO reaction (Tian et al., 2015). The induction period is also critical for MTO reaction. The induction period is a stage during which the organic-free zeolite catalyst is transferred to a working catalyst. Basically, the methanol conversion in the induction period could be quite low, which is controlled by the complicated reaction kinetics of element steps (Qi et al., 2015). For DMTO catalyst, the induction period occurs at temperature below 350 °C (Yuan et al., 2012). Actually, the duration of induction period is a function of reaction temperature. This is important for instructing the operation of industrial DMTO reactors, where the reactor temperature has to be out of the range where the induction period occurs. In this regards, the quantitative incorporation of kinetic rates of the element steps into the reactor model is highly desired.

3.2 Reaction–Diffusion at Catalyst Scale

It has been well known that the topology (i.e., pore size, cavities, and pore network) and composition (i.e., acidity strength and acid sites distribution) of zeolite particles can affect the product distribution. One interesting finding is that SAPO-34 zeolite used in DMTO process shows a higher selectivity to ethylene with certain coke deposition. The mechanism underlying this finding is discussed in Section 5. Anyway, a simple explanation is that the pore blockage due to coke formation inhibits molecular diffusion in the pore channel (Guisnet, 2002), which in turn leads to an intense restriction for larger molecules to diffuse out of the cavities. However, it should be noticed that the coke deposition may cause some acid sites to be covered, and, in serious cases, make the zeolite particles deactivated rapidly. It is thus expected that the optimal coke deposition exists for SAPO-34 zeolite particles, by which a high selectivity to ethylene can be achieved while the catalyst is still not deactivated. The understanding of this shape selectivity in DMTO reaction requires a detailed study on the diffusion and reaction inside SAPO-34 zeolite particles. However, *in situ* measurements of the

detailed diffusion and reaction inside SAPO-34 zeolite particles, if not impossible, would be extremely difficult. In this regards, the modeling approach seems to be much feasible.

An industrial DMTO fluidized bed catalyst pellet is basically composed of SAPO-34 zeolite particles and catalyst support (or matrix). The pores of zeolite particles and matrix are interconnected as a complex network. The pores inside zeolite particles are typically micropores (less than 2 nm) and the matrix normally has either mesopores (2–50 nm) or macropores (>50 nm), or both (Krishna and Wesselingh, 1997). The bulk diffusion coefficients in the meso- and macropores might be several orders of magnitude larger than surface diffusion coefficients in the micropores. Kortunov et al. (2005) found that the diffusion in macro- and mesopores also plays a crucial part in the transport in catalyst pellets. Therefore, other than a model for SAPO-34 zeolite particles, a modeling approach for diffusion and reaction in MTO catalyst pellets, which are composed of SAPO-34 zeolite particles and catalyst support, is needed.

3.3 Reaction and Solid–Gas Flow at Reactor Scale

The DMTO catalyst pellets are typically A type according to Geldart's classification in terms of fluidization characteristics (Tian et al., 2015). For this type of particles, the fluidization regime in the reactor can change from homogeneous fluidization to bubbling fluidization and turbulent fluidization, and to fast fluidization when the superficial gas velocity increases. Besides, the increase of reactor size also leads to significant variation of solid–gas two-phase flow patterns. The inelastic collisions between catalyst pellets lead to the formation of heterogeneous structure such as catalyst clusters. The intrinsic bubbling behavior in fluidized bed intensifies gas bypass and weakens the mass transfer in the reactor. The catalyst clusters and gas bubbles could further develop with an increasing reactor size or a higher gas velocity, which complicates the scaling up process of MTO fluidized bed reactor. The DMTO fluidized bed reactor was scaled up via various experiments at four different scales (Tian et al., 2015). The scale factor between two adjunct scales is roughly 100 in terms of methanol feed rate, and 10 in terms of reactor diameter. The microscale fluidized bed was operated at bubbling fluidization regime without catalyst circulation. In the pilot-scale experiments, the circulation between reactor and regenerator was established. In the demonstration and commercial scale, the turbulent fluidized bed reactor has been selected in order to achieve a high feed throughput.

As discussed above, the diversity of hydrodynamics in the reactors of different scale is one of the big challenges encountered in the fluidized bed scale-up, which has also been well addressed by a few researchers (Knowlton et al., 2005; Matsen, 1996; Rüdisüli et al., 2012). Another challenge that has been seldom discussed is about the translation of experimental results obtained from microscale DMTO fixed fluidized bed experiments to pilot-scale circulating fluidized bed reactor design and operation. In the microscale DMTO fluidized bed reactor, the catalyst is not circulated for regeneration. Thus, the coke content in catalyst increases with time on stream (TOS). But at any given time, the coke content can be considered as uniformly distributed in space because of the excellent mixing of solids in fluidized bed, which is shown in Fig. 6. However, in pilot-scale reactor, the catalyst is transported continuously to the regenerator to restore the activity by burning off the coke deposited on the catalyst. The regenerated catalyst with almost zero coke content is then transported back to the reactor. Figure 7 shows the typical distribution of coke content in catalyst in pilot-scale circulating fluidized bed reactor, which is not uniform in space due to the non-homogeneity of the residence time of catalyst in the fluidized bed. From Figs. 6 and 7, it can be seen that the coke distribution in the circulating fluidized bed differs significantly from that of fixed fluidized bed. Note that the coke content in catalyst is the key to achieve a high selectivity to ethylene, the translation of the microscale fluidized bed results to the circulating fluidized bed design actually represents a critical step in scaling up the DMTO reactor.

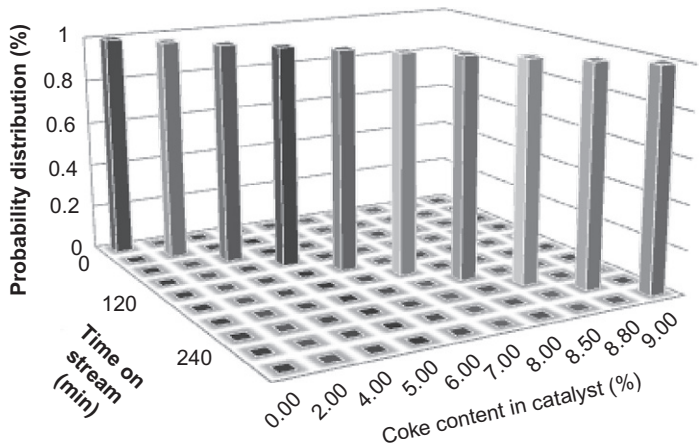

Figure 6 Typical distribution of coke content in catalyst in microscale DMTO fluidized bed reactor.

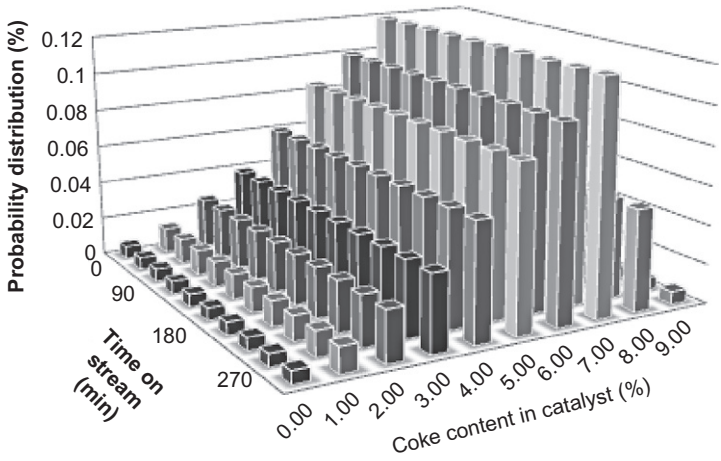

Figure 7 Typical distribution of coke content in catalyst in pilot-scale DMTO fluidized bed reactor.

3.4 Mesoscale Studies: The Key in MTO Process Development

In the DMTO process development, as discussed above, there were some specified issues at different scales. These issues are critical for instructing the scaling up, design, and operation of the fluidized bed reactor. The solutions to these issues, however, require knowledge and information obtained from a more fundamental scale. Quantitative translation of the knowledge and information from a lower (i.e., the characteristic size is smaller) scale to the issue of interest (normally at a higher scale) is actually the task of the mesoscale studies as proposed by Li et al. (2013). For example, in DMTO reaction mechanism study, the simulation results of QM can be used in MD only if the influences of topologies and morphologies of zeolites have been investigated and understood. In this chapter, the mesoscale challenges and the related studies in the DMTO process development are illustrated and discussed. Particularly, we focus on three aspects: a mesoscale modeling approach for MTO catalyst pellet, coke formation and control in MTO reactor, and scaling up of the microscale-MTO fluidized bed reactor to pilot-scale-fluidized bed reactor.

4. MESOSCALE MODEL FOR MTO CATALYST

4.1 Microscale Modeling for Reaction–Diffusion in Zeolites

The understanding of reaction–diffusion process in MTO catalyst pellet is of great importance in catalyst design optimization, and, as discussed above,

understanding the coking behavior. A single DMTO catalyst pellet could be considered composed of microporous SAPO-34 zeolite particles and catalyst support (or matrix). The overall performance of a single catalyst pellet is dependent on both reaction–diffusion process of the zeolite crystal region and diffusion process of support region. Basically, the zeolites are active part of the pellet and the reactions mainly occur in this part.

As the online measurement of the reaction and diffusion inside a single zeolite particle is still not realistic, mathematical modeling offers an alternative way for describing the reaction–diffusion process in zeolite region. A reliable model should reveal the physical essence of the reaction–diffusion process. In principle, quantum chemical or *ab initio* dynamical simulation may provide the accurate prediction to the catalytic reaction process. But the quantum chemical approach is very time-consuming and mainly simulates the energy barriers of elementary reactions and vibration frequency spectrum of stationary geometries (Hansen and Keil, 2012; Keil, 2012), which prevents it from direct application in catalyst design and reactor optimization. A hierarchical multiscale approach by Keil (2012) and Hansen and Keil (2012) combined different approaches such as first principles, quantum chemistry, force field simulations and macroscopic differential equations to simulate the active centers of the catalyst, adsorption and diffusion of reactants and products, and reaction and diffusion in zeolite particles and fixed bed reactors, respectively. In this approach, the continuum model could be naturally constructed when the chemical kinetic and diffusion parameters are derived from lower scales.

This continuum model could be applied to describe reaction–diffusion process in zeolite region (or zeolite crystal particle). We call this model microscale model. In this model, the partial differential equations (PDEs) used to describe the change of loading with time of species i in zeolite region are expressed as (Li et al., 2015a)

$$\frac{\partial q_i}{\partial t} = -\nabla \cdot \vec{N}_i + r_i \quad (i = 1, 2, \ldots, n) \tag{1}$$

where q_i is the loading of species i, $\vec{N}_i$ the molecular flux of component i, and r_i the reaction rate of species i. And the molecular flux is calculated based on Maxwell–Stefen theory (Krishna and van Baten, 2009):

$$\begin{pmatrix} \vec{N}_1 \\ \vec{N}_2 \\ \vdots \\ \vec{N}_n \end{pmatrix} = -[B]^{-1}[\Gamma] \begin{pmatrix} \nabla q_1 \\ \nabla q_2 \\ \vdots \\ \nabla q_n \end{pmatrix}. \tag{2}$$

The detailed defines of matrix [Γ] and matrix [B] could be found in Li et al. (2015a). It is noted that the diffusion of each species, based on Eq. (2), is coupled by all other species.

This micromodel could be used to investigate the effect of zeolite particle size on its catalytic performance. The influence of crystal size actually represents the impact of species diffusion on the reaction, and could be quantified by the internal effective factors, which are defined as following

$$\eta_{Z,i} \equiv \frac{\int_{V_Z} r_i \mathrm{d}V + \frac{c_u^s}{c_u^v}\int_{S_Z} r_i \mathrm{d}S}{r_i^b V_Z} \tag{3}$$

where V_Z represents the total volume of zeolite region, and S_Z is the total area of the boundary faces of zeolite region, and r_i^b is the reaction rate of species i calculated at the region boundary condition. c_u^s means the number of unit cells per square meters, and c_u^v represents the number of unit cells per cubic meters.

Despite the development of microscale modeling for reaction–diffusion in zeolite, the complex of MTO reaction mechanism impedes the application of microscale modeling to MTO process. Up to now, the reliable reaction kinetics based on element reactions in MTO process is still under development (van Speybroeck et al., 2014). However, a reduced or simplified microscale model could be applied. Basically, the diffusion effect is negligible if the crystal radius is small enough. Then mass equation, i.e., Eq. (1), could be simplified by neglecting the species flux term. In this case, MTO processes over ZSM-5 and SAPO-34 catalyst could be simulated by use of the single-event kinetics by Alwahabi and Froment (2004a) as an input.

4.2 Macroscale Modeling for Reaction–Diffusion in MTO Reactor

Methanol transformation to olefins over SAPO-34 catalyst is featured by high exothermicity (Alwahabi and Froment, 2004b) and rapid deactivation (Chen et al., 1999; Park et al., 2008). Considering these, circulating fluidized bed is used for MTO process in industry. The model describing reaction–diffusion process in this macro reactor is called macroscale model. However, it should be pointed out that the focus of macroscale model on reaction and diffusion is far different from microscale model.

In microscale model, the reaction kinetics is constructed on the basis of element reaction system, and usually could be obtained by quantum

chemistry calculation and transition theory. It means that the reaction kinetics in the microscale model is mainly determined by the structures of zeolite and reaction species, and is independent of other conditions, such as the size of catalyst particles. Such reaction kinetics has its corresponding appropriate computational unit. For example, the effective factor for alkylation of benzene over H-ZSM-5 crystal, as described above, is sensitive to computational unit in the size range of 0.1–1 μm. It is obvious that macroscale model of MTO reactor could not afford such a heavy calculation by using computational unit of this size. Therefore, the ensemble-average (or effective) reaction rates and simplified reaction network are normally used in the chemical kinetics in macroscale model. The parameters of chemical kinetics in macroscale model could be derived via two schemes: one is based on the simulation results from microscale models and another one is lumped from experimental data. As in the first scheme, the simulations can be considered as virtual numerical experiments. These two schemes, at first glance, show some similarity. However, the first scheme exhibits several advantages over the second scheme. The simulation methods used in the first scheme include exclusively quantum chemistry and MD, which have solid theoretical foundations. The second scheme is mainly dependent on the experimental conditions and, to certain extend, the researchers' experience. In addition to that, in numerical experiments, the effect of fluid flow and/or diffusion on reaction kinetics in the reactor could be readily reduced by incorporating well-designed simulations conditions. Such ideal conditions, in general, could not be achieved in realistic experiments. Thus the first scheme, in many cases, is much more efficient. However, the second scheme is still widely employed by researchers due to the complexity of MTO reaction process.

Since in the macroscale model, the reaction rate and diffusion coefficient are effective ones that are obtained on an ensemble-averaged basis, the internal diffusion will not appear in the controlling equations explicitly. The effective reaction rate already includes the influence of internal diffusion inside catalyst pellets. The external mass transfer term, which mainly accounts for the species transport outside catalyst pellets, is used in the controlling equations in macroscale models. So, the diffusion mentioned in macroscale model normally represents species diffusion outside catalyst pellets. In fluidized bed, species diffusion is closely related to the flow regime in the reactor (Abba et al., 2003). Abba et al. (2003) summarized the formulae for calculating diffusion coefficients in different flow regimes in fluidized bed.

If the effective reaction rates and diffusion coefficients are known, the mass equation of reaction species i in fluidized bed could be written as following:

$$\frac{\partial\left(\varepsilon_g\rho_g m_{g,i}\right)}{\partial t}+\nabla\cdot\left(\varepsilon_g\rho_g\vec{v}_g m_{g,i}\right)=\nabla\cdot\left(\varepsilon_g\rho_g D_{g,i}\nabla m_{g,i}\right)+R_i. \quad (4)$$

When Eq. (4) is coupled with controlling equations of mass and momentum for gas phase and solid phase, the detailed flow-reaction–diffusion process in a MTO fluidized bed reactor can be simulated (Zhao et al., 2013). In practical applications, simplified models for two-phase hydrodynamics are also proposed (Abba et al., 2003; Bos et al., 1995; Zhang et al., 2012), in which the detailed flow patterns cannot be calculated but it is very efficient in the overall reactor performance evaluation.

Despite the controlling equations used in macroscale models for MTO process, another important issue needs to be considered is the reaction term. In MTO process, the coke deposits increasingly on catalyst particles with TOS, and the reaction rate changes correspondingly. When the coke accumulates to a certain amount, the activity of catalyst will become lower. In real industrial MTO unit, the spent catalyst with certain coke deposition in the reactor is transported to regenerator via standpipes. And a large portion of coke on the catalyst is burned off in the regenerator, and these regenerated catalyst particles, which have sufficient reaction activity, then will be returned to the MTO reactor. In fact, the catalyst particles in MTO reactor stay in a dynamic balance due to the continuous outflow of spent catalyst and inflow of regenerated catalyst. This indicates that the residence time of catalyst in the reactor shows a certain distribution. Note that the coke content on catalyst varies proportionally with residence time of the catalyst, the coke content on catalyst also demonstrates a distribution in MTO reactor, which means that different catalyst particle in the reactor may have different coke content. Therefore, the correct formula of reaction term in mass equation should be expressed as $\int_{C_{C,ini}}^{C_C,\max} p\left(C_C, C_{C,ini}\right)\cdot r_i(C_C)\mathrm{d}C_C$, where $C_{C,ini}$ is the initial coke content on catalyst, $C_{C,max}$ is the maximum coke content on catalyst, and $p(C_C, C_{C,ini})$ is the probability density function of coke content on catalyst. The variable C_C is the coke content on catalyst particle, and function $r_i(C_C)$ is the reaction rate of species i. By assuming that $p(C_C, C_{C,ini})$ is independent of space

coordinates, we can derive the following expression based on the population balance theory:

$$p\left(C_{\mathrm{C}}, C_{\mathrm{C,ini}}\right) = \frac{1}{\tau \cdot r_{\mathrm{coke}}\left(C_{\mathrm{C}}\right)} \exp\left(-\int_{C_{\mathrm{C,ini}}}^{C_{\mathrm{C}}} \frac{1}{\tau \cdot r_{\mathrm{coke}}\left(C_{\mathrm{C}}\right)} \mathrm{d}C_{\mathrm{C}}\right) \tag{5}$$

where τ indicates residence time of catalyst particles in MTO reactor.

Another approach accounting for the influence of coke content distribution is to use the age distribution of catalyst particles (Bos et al., 1995; Zhang et al., 2012). Suppose that the catalyst particles are perfectly mixed, the age distribution of catalyst particles is

$$E(t) = \frac{1}{\tau} \exp\left(-\frac{t}{\tau}\right) \tag{6}$$

where t is time. Then average rate constant and average coke content can be described as in the following forms:

$$\bar{k}_i = \int_0^{\infty} k_i\left(C_{\mathrm{C}}(t)\right) E(t) dt \tag{7}$$

$$\bar{C}_C = \int_0^{\infty} C_{\mathrm{C}}(t) E(t) dt \tag{8}$$

Both approaches on reaction terms discussed above could give the same results. However, the coke distribution approach based on the population balance theory shows the physical picture in a much clear way. By introducing coke content distribution or age distribution of catalyst particles in the controlling equations, the flow-reaction–diffusion process in MTO reactor could be simulated more realistically.

4.3 Mesoscale Modeling for Reaction–Diffusion in Catalyst Pellet

Apparently, there lacks an explicit link between the microscale and macroscale models discussed above. In this section, a mesoscale model is introduced to describe the reaction–diffusion in a single catalyst pellet. The significance of this model can be embodied at least in two aspects: a necessary link between the microscale model and macroscale model and the theoretical basis for MTO catalyst design optimization.

Before discussing the reaction–diffusion process over a single catalyst pellet, we should focus on the structure of the catalyst pellet first, as it is critical for the internal reaction–diffusion process. As mentioned above, an MTO

catalyst pellet is composed of zeolite regions and catalyst support (or matrix) regions. The support regions have meso-/macropores. And the zeolite regions are composed of small microporous crystal particles, which normally have micropores and are distributed discretely in the support regions. Figure 8 shows the sketch of the structure of an MTO catalyst pellet. Reactions occur mainly in the zeolite regions, and species transport occurs in both zeolite and catalyst support regions. However, the diffusion mechanisms are different due to the difference of pore sizes. For microporous crystal particles, surface diffusion of adsorbed molecular species along the pore wall surface is dominant. For meso-/macropores, the bulk or molecular diffusion and Knudsen diffusion are critical if no strong adsorption exists. When there is a net change in the number of moles inside the porous catalyst pellet, the internal pressure gradient is always not negligible and this pressure gradient leads to viscous or Darcy flow (Krishna and Wesselingh, 1997). Figure 9 shows the schematic diagram.

The coefficients of bulk diffusion combined with Knudson diffusion in meso-/macropores is about 4 to 6 orders of magnitude higher than that of the surface diffusion in micropores, which means a large difference between the diffusion resistances of these two regions. It also implies that the difference of characteristic time of these two regions could be several orders of magnitude. The convenient approach to solve such a problem is to describe the reaction–diffusion processes in these two regions by two separate set of PDEs, which are coupling by the continuity of mass and heat flux for the same species at the interfaces.

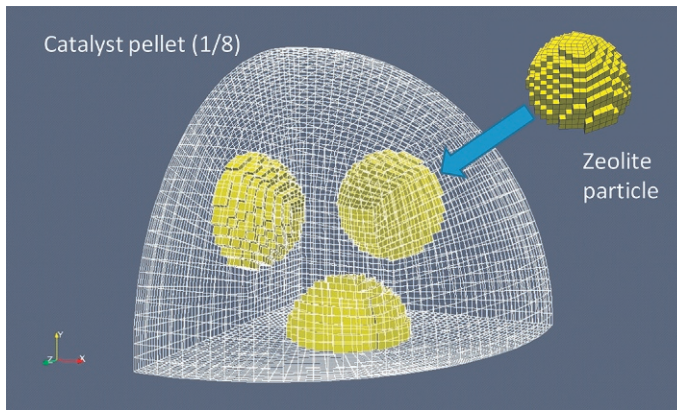

Figure 8 A catalyst pellet (1/8) formed with microporous zeolite particles and support regions.

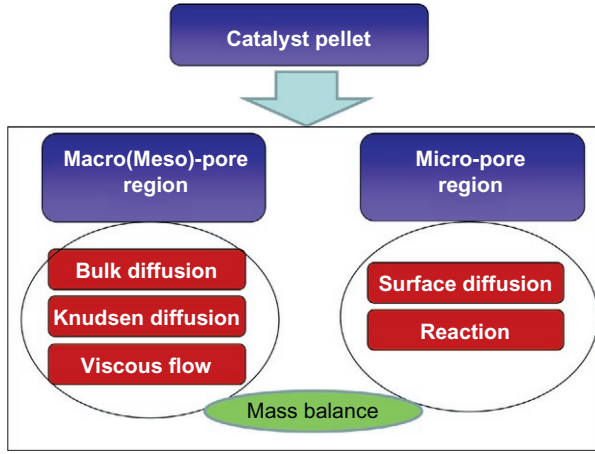

Figure 9 The schematic diagram of the mesoscale model for a single catalyst pellet formed with microporous zeolite particles and support regions (macro-/mesopore region).

For the zeolite regions, the reaction–diffusion process could be described by microscale model, as introduced above, since in these regions are mostly zeolite crystal particles. And for the support regions, the mass equation could be written as:

$$\varepsilon \frac{\partial c_i}{\partial t} = -\nabla \cdot \overrightarrow{\mathbb{N}_i} + \mathbb{r}_i \qquad (\mathrm{i} = 1,2\ , \ldots, \mathrm{n}) \tag{9}$$

where ε (in dimensionless) denotes porosity of catalyst support, c_i is the concentration of species i, $\overrightarrow{\mathbb{N}_i}$ is the molar flux of species i, and $\mathbb{r}_i$ is the reaction rate of species i. The value of $\mathbb{r}_i$ in the whole support region should be set to zero if the surface reactions are ignored. When incorporating the surface reactions, $\mathbb{r}_i$ should be set as zero in most cells. And only in the cells which are adjacent to the microporous crystal particles $\mathbb{r}_i$ needs to be calculated. The fluxes, $\overrightarrow{\mathbb{N}_i}$, could be given by (Li et al., 2015a):

$$\begin{pmatrix} \overrightarrow{\mathbb{N}_1} \\ \overrightarrow{\mathbb{N}_2} \\ \vdots \\ \overrightarrow{\mathbb{N}_n} \end{pmatrix} = -\left[\mathbb{B}^e\right]^{-1} \begin{pmatrix} \frac{1}{\mathrm{RT}} \nabla p_1 \\ \frac{1}{\mathrm{RT}} \nabla p_2 \\ \vdots \\ \frac{1}{\mathrm{RT}} \nabla p_n \end{pmatrix}. \tag{10}$$

The numerical methods have been developed for solving two sets of PDEs for two regions. This mesoscale model for a single catalyst pellet is called *multiregion model*.

The mesoscale model is of significant importance in catalyst design, since it could be used to investigate the effect of size, distribution, and amount of microporous crystal particles in the catalyst pellet on the overall catalytic performance. For convenience, as Eq. (3) in microscale model, another internal effective factor is defined to quantify catalytic performance of the pellet:

$$\eta_{\text{pellet},i} \equiv \frac{\int_{V_Z} r_i \mathrm{d}V + \frac{c_u^s}{c_u^v} \int_{S_Z} r_i \mathrm{d}S}{r_i^b V_{\text{pellet}}}. \tag{11}$$

It is meaningful to examine the relation between microscale model, mesoscale model, and micromodel. For reaction kinetics, microscale and mesoscale models adopt the same kinetics that based on element reaction system. For diffusion, mesoscale model embodies two diffusion mechanisms (one for micropores and another for mesopores and macropores), and microscale model considers one diffusion mechanism since it only has micropores. No diffusion was considered within the macropores. It is obvious that the mesoscale model possesses the same theoretical foundation as the microscale model, but its application scope has been enlarged compared to the microscale model. Therefore, it could be reliably used as a tool to derive some parameters, such as effective chemical kinetics and effective diffusion parameters, for macroscale model. In the section following, we discuss the method on how to link the microscale kinetics to the lumped macroscale kinetics via the mesoscale modeling approach.

4.4 Mesoscale Modeling: Linking the Microscale Kinetics and Macroscale Lumped Kinetics

4.4.1 Microscale Kinetics for MTO Reaction

In microscale model, the reactions generally refer to elementary reaction steps. The reaction network is closely related to the reaction mechanism and could be well obtained by quantum chemistry or *ab initio* calculations. The corresponding parameters, such as pre-exponential factors and activation energies, could be predicted based on transition state theory (TST) or variational transition state theory (VTST).

Although the MTO mechanism has been a topic of intensive research, the kinetics for elementary reaction steps is still a big challenge. The reaction

rate of elementary reactions is difficult to be measured due to the difficulty in separating the individual reaction of interest. There are always several or even more reactions occurring simultaneously, and these reactions may affect each other in a sophisticated way. In addition to that, the multi-compounds diffusion further complicates the derivation of reaction rate for elementary reactions. Among very few work for measuring reaction rate of the elementary steps, Svelle et al. (2005) reported their measurement of the methylation rate of alkenes by use of ^{13}C methanol and ^{12}C alkenes. Reaction conditions such as high flow rate and low contact time ensured that secondary reactions are minimized. Despite the reaction rates, the reaction paths for MTO process over SAPO-34 zeolites presents another challenge. The reactions in the zeolites are more difficult to be detected than that in gas phase. It is generally accepted that the hydrocarbon pool (Dahl and Kolboe, 1993), which has similar characteristics as the coke, includes intermediates that can react with methanol to form olefins. However, the intermediates likely vary with operation conditions as well as the structures of zeolites. Recently, polymethylbenzenes are supposed to be the reaction intermediates for primary olefins formation, and olefins are the intermediates for higher olefins formation. This mechanism shows two catalytic cycles, i.e., the aromatic carbon pool and olefin carbon pool (see Fig. 10; Bjorgen et al., 2007; Chen et al., 2012; Ilia and Bhan, 2013; Kumar et al., 2013). This dual cycle concept clearly increased our understanding on MTO reaction mechanism, thus prompts the development of the microkinetics.

Park and Froment (2001) proposed a detailed microkinetics for elementary reactions in MTO process over H-ZSM-5 catalyst, where the primary olefins formation was based on oxonium ylide mechanism, and higher

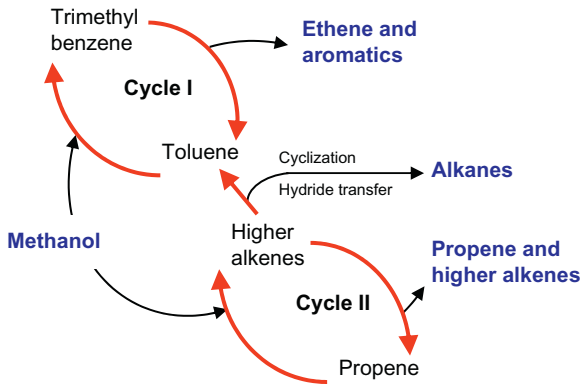

Figure 10 Dual cycle concept for the conversion of methanol over H-ZSM-5.

olefins formation was described in terms of carbenium ion chemistry. This microscale kinetic model was also applied to the MTO reaction over SAPO-34 catalyst by Alwahabi and Froment (2004a). Note that the primary olefins are formed through aromatic carbon pool cycle and higher olefins formed via the olefin carbon pool, Kumar et al. (2013) proposed a so-called single-event microkinetics for MTO process over H-ZSM-5 catalyst. The kinetic parameters are obtained by fitting the experimental data obtained at temperature from 643 to 753 K, space times between 0.5 and 6.5 kgcat*s/mol, and atmospheric pressure. Considering total number of elementary steps is large (318), the single-event concept combined with the Evans–Polanyi relationship was employed to reduce the number of kinetic parameters to be calculated. However, the kinetic parameters for elementary steps should be obtained via experiments with small catalyst particle size, and thus, the diffusion resistance could be safely ignored. When the diffusion plays a role within catalyst pellets in MTO process, the kinetic parameters are actually effective kinetic parameters rather than the intrinsic ones.

In principle, the microscale kinetics can also be obtained directly by quantum chemistry theory, TST or VTST theory, which, to a large extend, reflects the intrinsic kinetics for elementary reaction steps in MTO process. But so far, most of the theoretical calculations had only concentrated on part of the elementary reactions steps (Hemelsoet et al., 2011; Lesthaeghe et al., 2009; Van Speybroeck et al., 2011; Wang et al., 2010; Xu et al., 2013).

4.4.2 Macroscale Lumped Kinetics for MTO Reaction

The macroscale kinetics is usually based on several lumped compounds with simplified reaction network. The reaction rates were directly measured and the rate constants are ensemble averaged. On the basis of analysis of the kinetic data for the MTO process, Chen and Reagan (1979) suggested the three-lumped reaction kinetics with three reaction steps by considering autocatalytic reactions between methanol/dimethyl ether and olefins. Chang (1980) added one more reaction step and reaction species than Chen and Reagan (1979), and proposed four-lumped reaction kinetics for MTO process over ZSM-5 zeolites. In both models, olefins are lumped as a single reaction species. Schoenfelder et al. (1994) developed a seven-lumped kinetics by explicitly accounting for ethene, propene, and butane as three individual reaction species and incorporated corresponding reaction steps accounting for the formation of these olefins. Bos et al. (1995) considered the effect of coke on both activity and selectivity, and developed a kinetic model for MTO process over SAPO-34 catalyst. The model consists

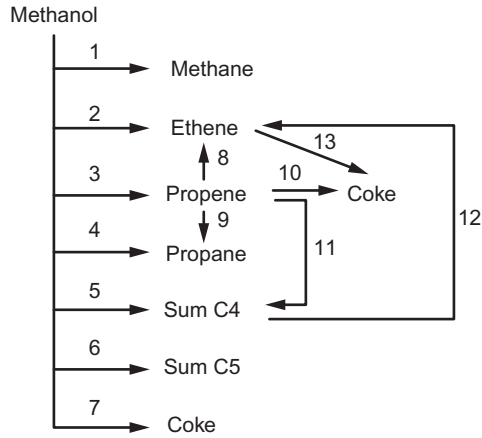

Figure 11 Kinetic scheme for MTO process over SAPO-34 catalyst by Bos et al. (1995).

of 12 reactions involving six species lumps plus coke (see Fig. 11), and the effect of coke on both the activity and selectivity is considered by using an empirical correlation for rate constants:

$$k_i(C_C) = k_i^0 e^{-\alpha_i C_C}, \tag{12}$$

where C_C is the coke content on catalyst. The effect of coke on the selectivity was predicted by taking different values for the empirical constant α_i. Another kinetic model for MTO process over SAPO-34 catalyst was proposed by Gayubo et al. (2000), in which the effect of water on activity and selectivity was included. Meanwhile, the model is further simplified by considering four individual steps for the production of ethylene, propylene, butylenes, and remaining hydrocarbons. The effect of water is described by multiplying a fraction term on rate constants:

$$\theta_W = \frac{1}{1 + K_W X_W} \tag{13}$$

where K_W indicates the resistance to species formation due to the presence of water and X_W represents the weight fraction of water. Recently, Ying et al. (2015) developed seven-lumped kinetic model for industrial catalyst in DMTO process. They proposed a new function to quantify the effect of coke on the activity and selectivity of DMTO catalyst

$$\phi_i = \frac{1}{1 + A\exp\left(B \times (C_C - D)\right)} \exp\left(-\alpha_i C_C\right). \tag{14}$$

Here, A, B, D, and α_i are empirical constants.

In actual applications, a simpler kinetic model is more favored for large-scale reactor simulation, suppose that it can adequately describe the reaction and transport process in the reactor. The simplification is normally based on the experimental findings. For example, Gayubo et al. (2000) reduced the number of reactions from eight to four by eliminating some reaction steps with slow reaction rates. Therefore, the application scope of the macroscale reaction kinetics is highly dependent on the experimental conditions studied.

4.4.3 Mesoscale Modeling: Linking the Microscale Kinetics and Lumped Kinetics

As mentioned above, in the macroscale kinetics, the reaction rate constants are ensemble averaged, and, in most of cases, representing gross effect of reaction rates for elementary steps and the corresponding mass transfer. This can be well explained by Eqs. (3) and (11). If the surface reactions are negligible, $\eta_{Z,i}$ and $\eta_{\text{pellet},i}$ could be viewed as the ratios of volume-averaged reaction rate to elementary step rate for zeolite crystal particles and catalyst pellet, respectively. The $\eta_{Z,i}$ and $\eta_{\text{pellet},i}$ become smaller if the diffusion is of increasingly importance. So the microscale kinetics in most situations may not be directly compared to the macroscale experimental results, if the internal and external diffusion cannot be accounted for. Using catalyst of smaller size might reduce the diffusion resistance to certain extend in kinetic study.

The mesoscale multiregion model discussed above may open a way to link the microscale kinetics to the macroscale kinetics. The macroscale kinetics derived from microscale kinetics at least ensures that the reaction mechanism at the microscale can be correctly reflected. As mentioned by Campbell (1994), knowing a mechanism can give an intelligent way to extrapolate kinetics to unknown conditions. As far as we know, there is no MTO macroscale kinetics at present derived directly from microscale kinetics.

It is also possible to carry out detailed study on the reaction and diffusion process at catalyst pellet scale. Different diffusion–reaction mechanisms, as well as the microscale kinetics can be implemented in the zeolites and support regions through the multiregion model, as described above. By considering the realistic size and distribution of zeolite crystal particles, we can simulate the reaction–diffusion inside a single catalyst pellet. A direct numerical simulation (DNS) approach is also under development in the authors' group to study the catalyst–gas interaction. The mesoscale multiregion modeling approach, if coupled with the DNS method (Van der Hoef et al., 2006), may eventually compute the lumped kinetic parameters. We

would stress, however, the application of the mesoscale model approach in MTO process is still far from being reached because of the complexity of MTO reaction.

5. COKE FORMATION AND CONTROL FOR MTO PROCESS

MTO reaction mechanisms over SAPO-34 catalyst have been investigated by many researchers (Olsbye et al., 2012). The formation of coke species can be readily occurring in MTO process over SAPO-34 catalyst. Here, the species of coke refers to the carbon depositions that can plug the pore and cover the active centers. However, in acidic molecular sieve-catalyzed reactions including methanol transformation reaction, the molecules cannot diffuse out of the channels and stay in the channels or cages if the molecular size is too large or the molecules have strong proton affinity. On one hand, this prompts the selectivity to smaller molecules that can diffuse out of the channels, for example ethylene. On the other hand, the accumulation of large molecules components would limit the mass transfer of reactant and accelerate the coverage of acidic centers, causing side reactions and catalyst deactivation. Apparently, coke formation is not only the major cause of deactivation in MTO reaction but also decisive to the light olefins selectivity. The understanding of coke formation and its control in MTO process is of practical importance. But the coke formation over zeolite catalyst is essentially a multiscale phenomenon. Froment (1997) proposed that the coke formation and catalyst deactivation could be studied at three scales: microscale for activity center such as acid center inside channel, pore or cage of zeolites; mesolevel for topology of zeolite such as pore, channel, or cage; and macrolevel for reactor.

5.1 Coke Formation at Microscale: Effect of Acidity of Catalyst

The acidity of the catalyst has a significant effect on the deactivation of the catalyst. Researches by Wilson and Barger (1999), Mores et al. (2011), and other research groups (Dahl et al., 1999a,b; Haw, 2002; Stocker, 1999; Yuen et al., 1994; Zhu et al., 2008) discovered that the catalyst with a strong acidity and higher acid center density has higher deactivation rate in MTO reaction. Guisnet et al. (2009) related the catalyst acidity to chemical reaction rate, as shown in Fig. 12. The stronger the acidity of catalyst, the higher the reaction rate in MTO process. In this case, the coke precursor formation, and thus, the coke deposition accelerates. This in turn prompts catalyst deactivation. In addition to the acidity, the density of acid sites on

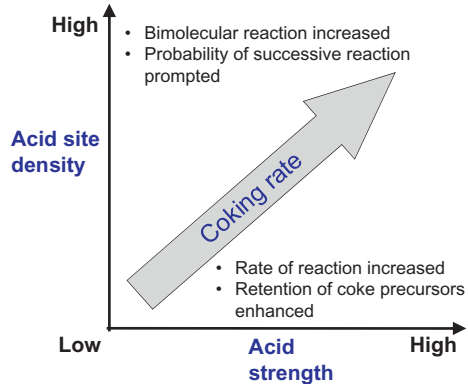

Figure 12 Influence of the acidity and acid site density in catalyst on the rate of coking.

the catalyst also plays a crucial role in catalyst deactivation. A higher density of acid sites normally means shorter distance between two adjacent acid centers. In this case, the reactant molecules under diffusion in channels and cages may have higher probability to be absorbed by acid centers, react, and generate coke species. Therefore, the catalyst deactivation rate is also enhanced with a higher density of acid sites.

Yuen et al. (1994) have compared the methanol conversion over SAPO-34 and H-SSZ-13 catalyst, which have same CHA topology, density of acid sites, and grain size. The results show that H-SSZ-13 has higher deactivation rate owning to its higher acid strength. Under the same temperature, the coke species on SAPO-34 catalyst are mainly methyl benzene and methyl naphthalene, while on H-SSZ-13, the monocyclic, bicyclic, and tricyclic aromatic hydrocarbons and their derivatives are observed. It is suggested that the polycyclic aromatic hydrocarbons can be generated more easily in methanol conversion over H-SSZ-13 than that over SAPO-34 due to the difference of acid strength of zeolites.

5.2 Coke Formation at Mesoscale: Effect of Topological Structure of Zeolites

In methanol conversion over molecular sieves having three-dimensional pore and cage structures, methyl benzene is recognized as a reactive intermediate that can enhance the reaction rate, and the bicyclic aromatic hydrocarbons show very low activity in prompting methanol conversion. Actually, both the bicyclic and polycyclic aromatic hydrocarbons can be coke species during catalyst deactivation in MTO process over molecular sieves (Wei et al., 2012a). The formation of polycyclic aromatic

hydrocarbons requires a certain spatial structure inside the molecular sieves. Therefore, the formation of main components of coke should be closely related to the topology of molecular sieves in MTO process.

The different topology structures of ZSM-5 and SAPO-34 lead to different deactivation modes during the conversion of MTO. ZSM-5 molecular sieve has smaller 10-ring cross channel, which cannot provide sufficient space to allow the formation of macromolecular bicyclic aromatic hydrocarbons and polycyclic aromatic hydrocarbons. The channels can only allow generating relatively small number of methyl benzene. And these species are able to diffuse from 10-ring pore channel to the gas phase. The channel structure of ZSM-5 decides the coke species generation (Bjorgen et al., 2007). The deactivation of ZSM-5 in MTO reaction is mainly caused by coke deposition on outer surface (Fig. 13A; Guisnet et al., 2009).

SAPO-34 has small 8-ring channels and big cage structure. Methyl benzene, the intermediates in MTO process, can be converted to polycyclic aromatic hydrocarbons in the cage. As the polycyclic aromatic hydrocarbons have large volume and occupy most of the space in the cage, which hinders the contact between methanol molecules with the active sites and reduces the mass transfer rate substantially (as shown in Fig. 13B), the catalyst will lose the activity rapidly (Haw et al., 2003). The study of Hereijgers et al. (2009)

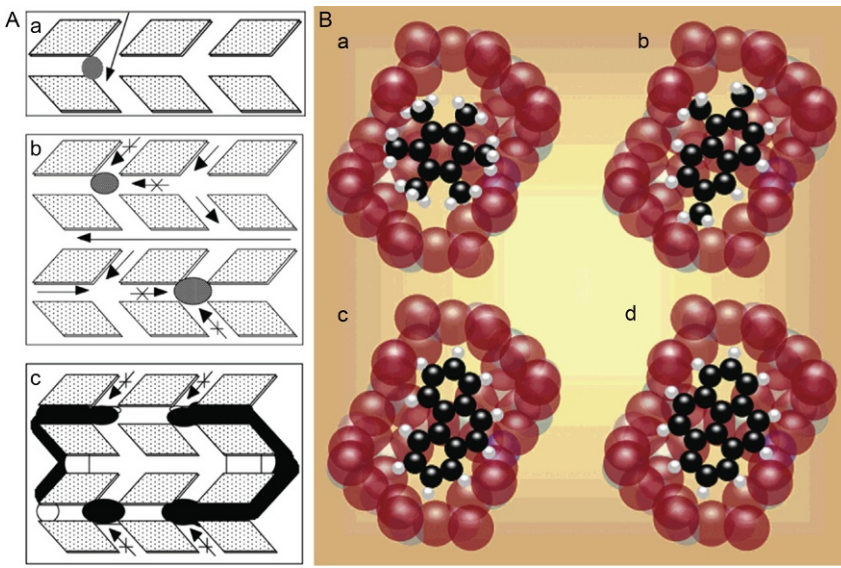

Figure 13 Deactivation process in MTO reaction over ZSM-5 (A) (Guisnet et al., 2009) and SAPO-34 (B) (Haw et al., 2003) zeolites.

also supports that low diffusion rate can cause the deactivation of SAPO-34 catalyst. Due to the restriction of the opening of 8-ring window, it is difficult for large molecules to move out of the channels in SAPO-34 zeolites, and thus, the heavy compounds of coke can be readily accumulated in MTO reaction. Mores et al. (2008) have studied the coke formation in SAPO-34 and ZSM-5 zeolites in methanol conversion process by use of *in situ* measurement techniques and confirmed the difference between these two catalysts.

Bleken et al. (2011) have compared the methanol conversion of four kinds of catalysts with 10-membered ring three-dimensional pore structure (i.e., IMF, TUN, MEL, and MFI). They found that although all catalysts have 10-ring cross channel, but there are differences between them in terms of life time and coke compositions. Since the cross channels in IMF and TUN structure have wide space near the cross, which allows the formation of heavy coke species, the zeolites (IM-5 and TUN-9) having IMF and TUN structure appear rapid deactivation in methanol conversion reaction. On the contrary, zeolites with MEL and MFI structure (such as ZSM-11 and ZSM-5), in which the space near the cross is relatively narrow and limits the formation of coke compositions, have a long life time in the methanol conversion reaction. In this case, there are no heavy coke compositions in the channels, and the deactivation is mainly caused by the coke formation on external surface of zeolites.

5.3 Coke Formation at Mesoscale: Effect of Reaction Temperature

Schulz (2010) found that in MTO process over H-ZSM-5 catalyst, the operation temperature affects catalyst life time and deactivation mechanism significantly. At temperature of 543–573 K, large volume methyl benzene molecules (three methyl isopropyl ethyl benzene and two methyl benzene) may form and occupy the pores in H-ZSM-5 zeolites. While at a higher temperature of 625 K, these large volume methyl benzenes would be cracked into olefins and small volume benzene, and methyl benzenes, which may cause catalyst deactivation, do not exist in the channels of H-ZSM-5. When the temperature becomes higher than 625 K, coke generated at the external surface of H-ZSM-5 catalyst will be the dominant reason for catalyst deactivation. Bleken et al. (2009) have studied methanol conversion reaction and coke generation on two CHA cage structure zeolites, SAPO-34 and H-SSZ-13. They found that, by altering reaction temperature, the life time, coke content, and coke species show similar trend for these two

zeolites, although the acidic strength is different for Si–Al and Si–P–Al zeolites. If the reaction is kept at 573 K for 25 min,, the coke content of SAPO-34 zeolites can grow to 16%. When the reaction temperature is further increased to 673 K, the coke content drops to 6% in SAPO-34 zeolites. Under the same reaction conditions, the coke content in H-SSZ-13 zeolites first increases to 20% at 573 K, and then goes down to 9% at 673 K. Apparently, there is an optimized operation window for reaction temperature, which is from 573 to 698 K for both SAPO-34 and H-SSZ-13 catalysts. In this window, both catalysts have a relatively long life time. At an operation temperature departed from this range, catalysts may deactivate more quickly.

Yuan et al. (2012) investigated methanol conversion reaction and coke deposition over SAPO-34 catalyst in a microscale fluidized bed reactor, which presented some interesting results in their temperature-programmed experiments (Yuan et al., 2012). As shown in Fig. 14, methanol was fed to the reactor at 250 °C, but the hydrocarbon products generated in the temperature range of 250–300 °C is negligible. The conversion of methanol increased from temperature of 300 °C, and reached a peak conversion at 325 °C and then dropped until 350 °C. When the temperature further rose from 350 °C, the conversion of methanol increased continuously. In order

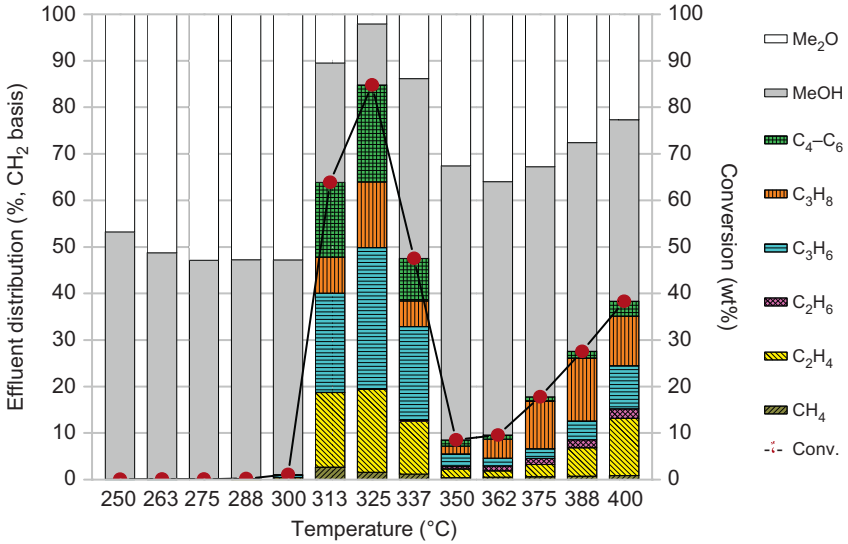

Figure 14 Effluent distribution of MTO process in a microscale fluidized bed reactor with temperature programmed (Yuan et al., 2012).

to understand this phenomenon, Wei et al. (2012a,b) studied the MTO reaction at constant temperatures, with a focus on the coke deposition and catalyst deactivation. Their results showed that methanol conversion reaction had distinguished characteristics at high and low temperature over SAPO-34 catalyst. At low temperature (<350 °C), the reaction is featured by an induction period, which may cause a fast deactivation of the SAPO-34 catalyst. The duration of the induction period is dependent on the reaction temperature. The higher the reaction temperature, the shorter the induction period. At high reaction temperature (>350 °C), catalyst deactivation is caused by rapid coke deposition. But in the range of 400–450 °C, the SAPO-34 catalyst has low coke formation rate and long life time, as shown in Fig. 15 (Wei et al., 2012b). The organic species of coke in the cage of SAPO-34 zeolites at high temperature are mainly fusing ring aromatic hydrocarbons, which attributes to the rapid deactivation of catalyst at high temperature but does not present at low temperature. Further researches show that at low temperature saturated alkane products such as adamantane compounds appears as coke species, as shown in Fig. 16 (Wei et al., 2012a). These adamantane compounds are different from methyl benzene and other aromatic coke species formed at high temperature. The latter can act as the hydrocarbon pool with functions of assembling C_1 compounds to higher hydrocarbons. These saturated naphthenic hydrocarbons occupy the cage and limit mass transfer of methanol molecules. Thereby, it suppresses the continuous formation of hydrocarbon pool species and results in rapid deactivation at low temperature.

Based on the results at constant temperature, it is possible to explain the peak conversion at 325 °C in the temperature-programmed experiments, as

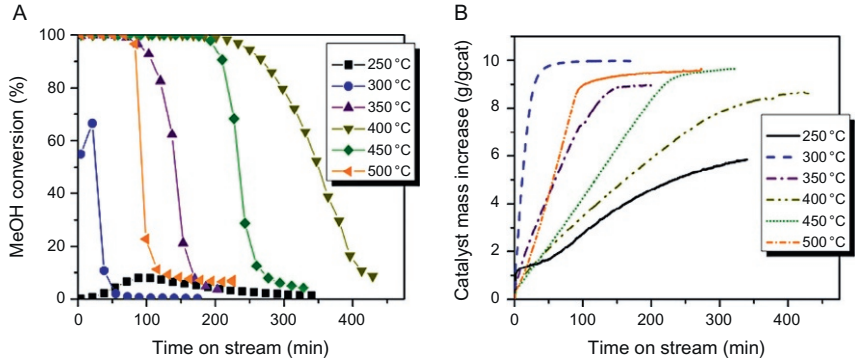

Figure 15 (A) Methanol conversion (■ 250, • 300, ▲ 350, ▼ 400, ◆ 450, and ◄ 500 °C) and (B) real-time catalyst mass increase observation (Wei et al., 2012a).

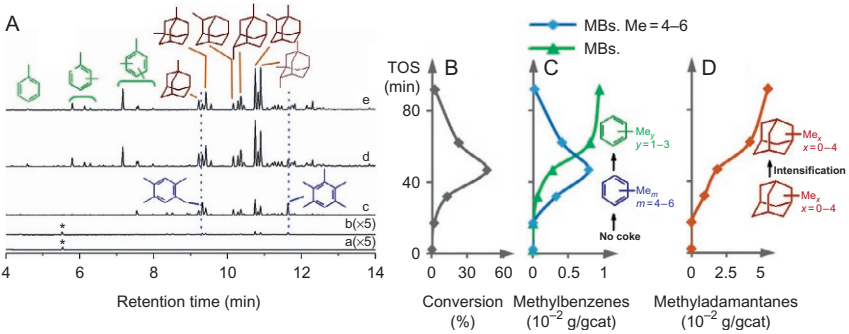

Figure 16 GC–MS analyses (A, left) of confined organics after methanol conversion at 300 °C for 17 (a), 32 (b), 47 (c), 62 (d), and 92 min (e). Methanol conversion with time on stream (B and C, middle) and confined methylbenzenes and methyladamantanes variation with time on stream (D, right) (Wei et al., 2012b).

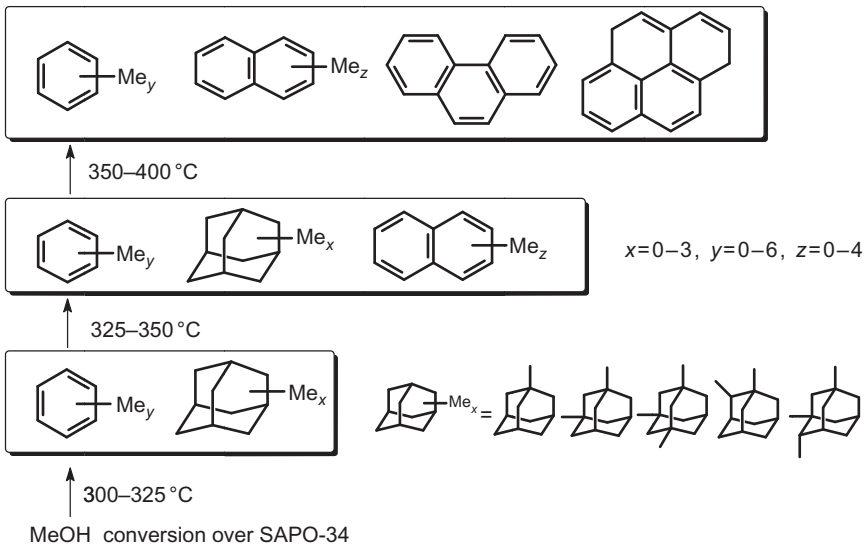

Figure 17 Coke species evolution in the temperature-programmed methanol conversion over SAPO-34 (Yuan et al., 2012).

shown in Fig. 14. At low temperature, the coke species is mainly adamantane species, and the formation and accumulation of which can lead to a rapid deactivation of catalyst. This species cannot act as hydrocarbon pool. When gradually increasing the reaction temperature, the adamantane compounds generated at low temperature are converted to naphthalene derivatives, and eventually form fused ring aromatic hydrocarbons phenanthrene and pyrene (Fig. 17). The coke species inside SAPO-34 zeolites

changes with temperature (Yuan et al., 2012), which complicates our understanding on coke formation in MTO process.

5.4 Coke Formation at Macroscale: Effect of Selectivity to Light Olefins

As discussed above, coke formation affects the selectivity to light olefins in MTO process over SAPO-34 catalyst. It has been found that at a given temperature, the ethylene-to-propylene ratio in MTO reaction is increased when coke content in catalyst increases (Barger, 2002; Song et al., 2001). Figure 18 shows the typical results in a microscale fluidized bed reactor at temperature of 450 °C and weight hourly space velocity (WHSV) of 1.5 h^{-1} without catalyst regeneration. As can be seen, when the coke content on catalyst increases from 2% to roughly 8%, the selectivity to ethylene increases from 37% to 48% while the conversion is still sufficiently high (>98.5%). The selectivity to propylene keeps almost unchanged. Thus, a gain of selectivity to light olefins can be achieved, with certain coke content on catalyst.

Two hypotheses have been proposed to explain this behavior: the first is that the accumulation of coke suppresses the free space in the cavities of zeolites thus limits the formation of methyl benzenes with 5–6 methyl groups, which thereby favors the ethylene formation. The second is that the diffusion of large product molecules from the cavities is hindered by partial blockage of pores and opening windows access to the cavities due to coke formation. Only smaller molecules such as ethylene can freely pass through

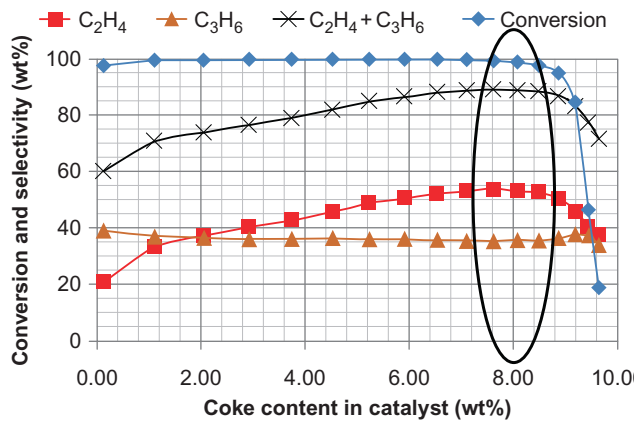

Figure 18 The methanol conversion and light olefins selectivity under different coke content on catalyst. Reaction temperature 450 °C, WHSV = 1.5 h^{-1}.

the partially blocked pores in SAPO-34 zeolites. Chen et al. (2007) studied the influence of coke content on the selectivity to different hydrocarbons. Their results clearly showed that the selectivity to ethylene increases with increasing coke content, and the selectivity to the following products drops to different extend with an increasing coke content: $C_6 > C_5 > C_4$. Dahl et al. (1999a,b) studied the product shape selectivity to olefins on different-sized crystals by use of ethanol and 2-propanol as probe molecules. It has been demonstrated that the diffusion of molecules is slow if the size of molecules is comparable to the channel size, which is named configuration diffusion. Dahl et al. (1999a,b) also found that ethanol conversion was not limited by the ethanol diffusion while 2-propanol conversion was controlled by 2-propanol diffusion. Barger (2002) has also proposed product shape selectivity by comparing the measured ethylene-to-propylene ratio with thermodynamically predicted ratio in the gas phase at different temperatures. It was found that the measured ethylene-to-propylene ratio was much higher than the thermodynamically equilibrium ratio.

5.5 Coke Control at Macroscale: Optimize the DMTO Fluidized Bed Reactor Design and Operation

In pilot-scale DMTO fluidized bed reactor, due to circulation of catalyst between reactor and regenerator, there exists a certain distribution of residence time of catalyst. Thus, the coke content on catalyst also shows a certain distribution, as shown in Fig. 7. But from Fig. 18, it is participated that, for a given temperature, an optimal value of coke content can be identified by which the selectivity to light olefins is maximized. Therefore, catalyst particles with coke content either higher or lower than the optimal value might lead to a lower selectivity to light olefins; the overall selectivity is then affected by the coke distribution in DMTO circulating fluidized bed reactor.

5.5.1 Counter-Current Fluidized Bed Configuration

In pilot-scale DMTO fluidized bed reactor, the regenerated catalyst normally has very low coke content. As discussed above, such catalyst may not favor the selectivity to light olefins. Therefore, a counter-current fluidized bed configuration is adopted. In this configuration, the regenerated catalyst is injected into the reactor via catalyst distributor from the top of the dense bed, and the coked catalyst is taken from the draw-off bin beneath the gas distributor at the bottom. Thus, the methanol feed from the gas distributor first contacts the coked catalyst, by which a higher selectivity to light

olefins can be achieved. Our experimental results confirmed that the yield of light olefins can increase by 5% when a counter-current configuration is used.

5.5.2 Minimize the Induction Period

At low temperature (<350 °C), the DMTO reaction is featured by an induction period, which may cause a fast deactivation of the SAPO-34 catalyst. Thus in the real operation, the induction period has to be avoided. Normally, the higher the reaction temperature, the shorter the induction period. Basically above 350 °C, the induction period can be minimized. Therefore, in the start-up of the DMTO reactor, the catalyst should be heated to above 350 °C before feeding methanol. Note that the organic species of coke in the cage of SAPO-34 zeolites at high temperature are mainly aromatics, which however are not found at low temperature; it is expected that the introduction of aromatics can shorten the induction period at lower temperature. Qi et al. (2015) showed that the induction period could be remarkably shortened by adding only 4 ppm of aromatics. This is very meaningful for DMTO reactor operation.

The coke formation is critical for MTO reaction over SAPO-34 catalyst. The influence of coke formation is twofold: a certain amount of coke deposition can prompt the selectivity to light olefins, while it also makes the catalyst deactivate rapidly. Thus, the understanding of the coke formation at microscale is extremely important for controlling coke distribution in the reactor. The influences of zeolite structure and reaction temperature on coke formation have been discussed to illustrate the essence of the mesoscale researches. However, there is still a lot of work to be explored at mesoscale concerning the coke formation. These results are eventually expected to benefit the reactor design and operation.

6. DMTO FLUIDIZED BED REACTOR SCALE-UP

Scale-up of fluidized bed has long been considered as a big challenge in catalytic reactor development (Knowlton et al., 2005; Matsen, 1996; Rüdisüli et al., 2012). On one hand, good understanding of the chemistry must be obtained. This includes the reaction mechanism, reaction kinetics, and catalysis behavior. On the other hand, the influence of hydrodynamics on the reactor performance plays another critical role (Knowlton et al., 2005). The hydrodynamics in fluidized bed has inherent multiscale nature. The fluidization behavior of catalyst can vary significantly with the change of

the physical properties (i.e., size and density) of catalyst particles and fluidizing gas (Geldart, 1973). The mild distribution of catalyst particles at microscale may lead to dynamic mesoscale heterogeneous structures such as bubbles and clusters, which are closely related to the fluidized bed size as well as the operation conditions. These dynamic mesoscale heterogeneous structures can further affect macroscale mixing and mass transfer in fluidized bed reactor (Sundaresan, 2013). In view of these complexities, scale-up of a new fluidized bed process, at current stage, is still an engineering practice rather than an exact science (Knowlton et al., 2005; Matsen, 1996; Rüdisüli et al., 2012).

DMTO fluidized bed reactor has been scaled up via experiments at four different scales (Tian et al., 2015). The scale factor between two adjunct scales is roughly 100 in terms of methanol feed rate, and 10 in terms of reactor diameter. The microscale fluidized bed was operated at bubbling fluidization regime without catalyst circulation. In the pilot-scale experiments, the circulation between reactor and regenerator was established. In the demonstration and commercial scale, the turbulent fluidized bed reactor has been selected in order to achieve a high feed throughput. One thing determined at the early stage of DMTO process development is that the DMTO catalyst particles should have similar physical properties as FCC catalyst particles. In this way, both DMTO catalyst and FCC catalyst are typical Geldart type A particles, which could maintain good fluidity in the fluidized bed operation. In previous reviews, such as Matsen (1996), Knowlton et al. (2005), and Rüdisüli et al. (2012), the challenges and general methods for scaling up fluidized bed reactor were summarized. Especially, these reviews specially focused on the influence of hydrodynamics in fluidized bed reactor scale-up. In this section, we intend to share our method on the analysis of the results at microscale and how to relate the microscale results to the design of pilot-scale fluidized bed reactor.

6.1 Microscale MTO Fluidized Bed Reactor

In the MTO process development, the purpose of microscale-MTO reactor experiments is threefold: (1) evaluation of the catalyst performance, (2) study of the influence of reaction conditions, and (3) exploration of the optimal reaction conditions that are used for pilot-scale reactor design. Due to the rapid deactivation of SAPO-34 catalyst and high exothermicity in MTO reaction, the fluidized bed reactor has been considered as the most suitable MTO reactor. In the laboratory, microscale-MTO fluidized bed reactor was

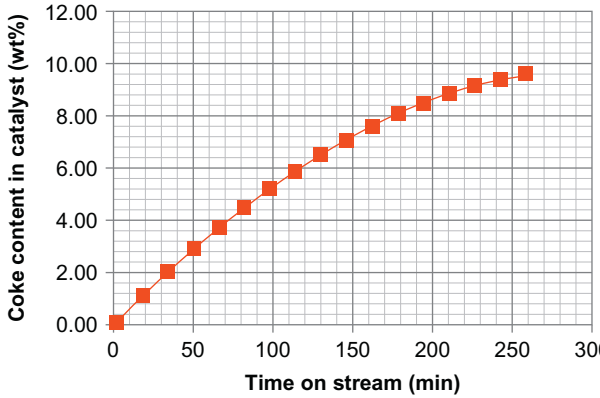

Figure 19 The coke content in catalyst as function of time on stream in microsale fluidized bed reactor. Reaction temperature 450 °C, WHSV = 1.5 h^{-1}.

constructed to study the reaction and kinetics. The notable difference between microscale fixed bed reactor and fluidized bed reactor is that the catalyst particles can be fluidized and well mixed in the latter. In the absence of circulation, the catalyst in microscale fluidized bed shows a uniform residence time distribution. And thus, the spatial distribution of coke content in catalyst, at any given time, can be considered as uniform. Figure 19 shows the typical results of coke content in catalyst (defined as the percentage of the mass of coke to the mass of catalyst) as a function of TOS. The corresponding methanol conversion and selectivity to ethylene and propylene are depicted in Fig. 18. Since there was no online regeneration, the coke content in catalyst experienced a continuous increase with the TOS in the microscale fluidized bed reactor until a considerably low conversion of 18.82% is achieved. A rapidly drop of methanol conversion was found at 210 min with a coke content in catalyst of 8.87%, which indicates that the activity of catalyst started to decline. In order to connect the results from microscale fluidized bed reactor to the pilot-scale fluidized bed reactor, important parameters, i.e., coke content in catalyst, coke formation rate, and catalyst-to-methanol ratio, have been studied.

6.1.1 Coke Content in Catalyst

In pilot-scale MTO experiments, the regeneration of spent catalyst deactivated in the MTO reactor was conducted in a continuous way by circulating catalyst from reactor to regenerator and vice versa. The activity of spent catalyst was then restored in the regenerator. When the steady circulation is established, and which is most likely the case in pilot experiments,

the average coke content in catalyst becomes time independent. The optimal average coke content in catalyst has to be known *in prior* to maximize the selectivity to ethylene and propylene while maintaining high methanol conversion. Typical results were shown in Fig. 18. As can be seen, under the conditions studied, the average coke content in catalyst of around 7.6–8.5% is favorable in terms of selectivity to ethylene and propylene (ca. 88–89%) and methanol conversion (>98.5%).

6.1.2 Catalyst Residence Time in Reactor

As mentioned above, the coke content in catalyst around 7.6–8.5% is favorable in terms of selectivity to ethylene and propylene (ca. 88–89%) as well as methanol conversion (>98.5%). Further check with Fig. 19, we can find that this is corresponding to the TOS of 160–195 min. Under the operation conditions specified in Fig. 19; therefore, a catalyst residence time of 160–195 min is optimal for light olefins selectivity in pilot-scale experiments. It should be noted that the WHSV influence the catalyst residence time significantly. An estimation of the catalyst residence time is based on $RT_1 = \beta \cdot RT_2 \cdot \mathrm{WHSV}_2/\mathrm{WHSV}_1$, where RT_i is the optimal catalyst residence time under WHSV_i, and β is the coefficient obtained from experiments. A simple estimation can be made by assuming β as 1.

6.1.3 Coke Formation Rate

Note that coke deposition in the MTO catalyst can lead to the coverage of part of the active sites and reduce the catalyst activity. When the coke content is sufficiently high, the methanol conversion shows a rapid decrease and most of the active sites have been covered and the catalyst becomes deactivated. From Fig. 18, we can find that in a wide range of coke content (0–8.87 wt%) the catalyst in the microreactor can maintain a high methanol conversion (>98.5%). This implies that the complete conversion of methanol can be realized with a small mass of active catalyst (and thus, a small amount of active sites) in MTO reaction. Therefore, it is important to know the coke formation rate in MTO process. Based on the data reported in Fig. 18, we can estimate the coke formation rate:

$$\dot{c}(t) = \frac{\mathrm{d}}{\mathrm{d}t}\left(W_{\mathrm{RX}} \cdot C_{\mathrm{cat}}(t)\right) = W_{\mathrm{RX}} \frac{\mathrm{d}}{\mathrm{d}t} C_{\mathrm{cat}}(t) \tag{15}$$

where W_{RX} is the catalyst loading in the microscale reactor and $C_{\mathrm{cat}}(t)$ is coke content. The coke formation rate, normalized by the catalyst loading, is shown in Fig. 20. As can be seen, the coke formation rate declines with an

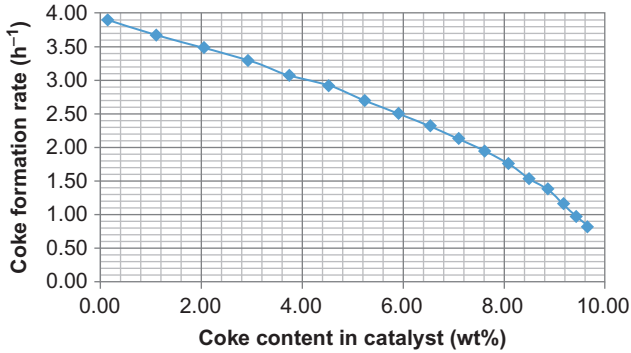

Figure 20 The coke formation rate as a function of the coke content. The coke formation rate is normalized by the catalyst loading, and the experimental conditions are the same as in Fig. 19.

increasing coke content in catalyst. This is not surprised since high coke content means more coverage of the active sites in catalyst, and thus a lower conversion of methanol. Lower conversion of methanol leads to a limited coke production.

6.1.4 Catalyst-to-Methanol Ratio

The third parameter of critical importance is the catalyst-to-methanol ratio. This parameter is the key to control the circulation rate of catalyst between reactor and regenerator in pilot-scale setup. Normally it is hard to derive the relation between the catalyst-to-methanol ratio and reaction results via direct measurement in the microscale experiments as there is no circulation. However, by analyzing the coke formation in the MTO reaction, we can predict the optimal catalyst-to-methanol ratio. From Eq. (15), we can obtain the coke formation rate. We assume that the coke formation rate can be directly used in the pilot-scale experiments. Thus, the mass flow rate of catalyst required to transport this amount of coke is estimated as following:

$$\dot{m}(t) = \frac{\dot{c}(t)}{C_{\text{cat}}(t)}. \tag{16}$$

And the cat-to-methanol ratio can be obtained as:

$$\text{CTM} = \frac{\dot{m}(t)}{\dot{Q}_m(t)} = \frac{\dot{c}(t)}{\dot{Q}_m C_{\text{cat}}(t)} \tag{17}$$

with $\dot{Q}_m(t)$ is the methanol feed rate. Figure 21 shows the methanol conversion and ethylene and propylene selectivity as a function of

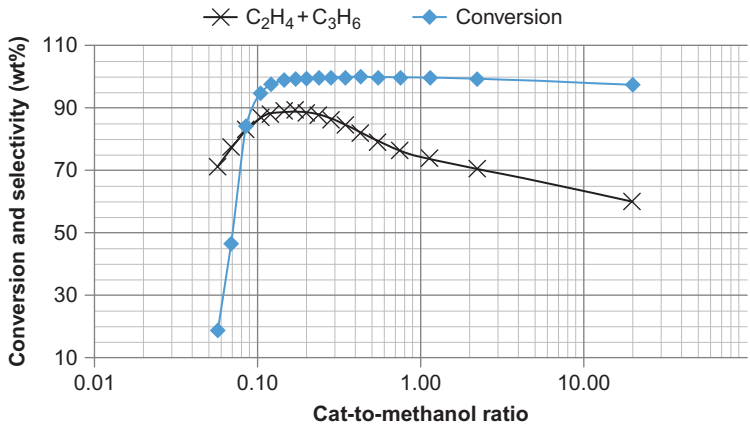

Figure 21 The cat-to-methanol ratio coke formation rate as a function of the coke content. The coke formation rate is normalized by the catalyst loading, and the experimental conditions are the same as in Fig. 19.

cat-to-methanol ratio. It is evidenced from Fig. 21 that there is an optimal operation window for light olefins selectivity in terms of cat-to-methanol ratio. The favorable cat-to-methanol ratio is 0.1–0.2, which can be used as the starting point for designing the pilot-scale MTO reactor.

It needs to be pointed out that the results discussed above may not necessarily be the same as in the pilot-scale experiments where the catalyst circulation between reactor and regenerator is established. The circulation of catalyst can maintain a steady average coke content but with certain distribution since the catalyst particles will have residence time distribution due to the back-mixing in fluidized bed. This will lead to the change of reaction results to certain extent. But the results obtained from microscale fluidized bed reactor can be used to guide the design and operation of pilot-scale setup.

6.1.5 Influence of Reaction Conditions

6.1.5.1 Reaction Temperature

It is well known that the methanol conversion process has induction period, which means that the methanol conversion cannot be 100% even with fresh MTO catalyst. The complete conversion of methanol will be achieved only after certain coke depositing on the catalyst. The duration of induction period is dependent on the reaction temperature. Figure 14 shows the results in the temperature-programmed reaction in the microscale fluidized bed reactor (Yuan et al., 2012). The reactor is first heated to 250 °C, and the

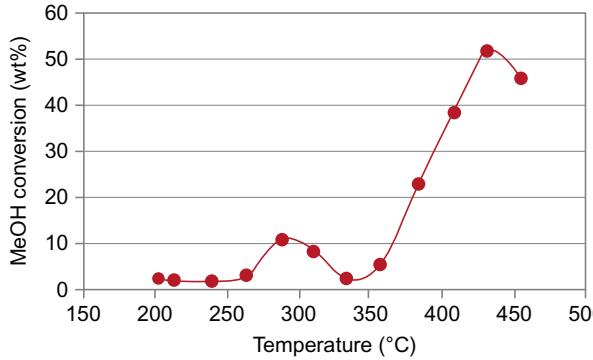

Figure 22 Temperature-programmed experimental results for coked catalyst in microscale fluidized bed reactor. Catalyst is pre-coked by reaction under 450 °C for 10 min. WHSV = 1.5 h^{-1} and water-to-MeOH ratio is 60:40 in the feed.

methanol is then fed in. Results show that from 250 to 288 °C, the product gas mainly contains methanol and dimethyl ether (DME). If we further increase the reaction temperature to 300 °C, light olefins such as ethylene, propylene, and butylenes start to appear in the product gas. The C_1–C_3 alkanes and C_4–C_6 hydrocarbons gradually increase when temperature rises from 300 to 325 °C. However, a significant drop of methanol conversion is found when we further increase the reaction temperature from 325 to 350 °C. The methanol conversion restores when the temperature is higher than 350 °C. Figure 22 shows the reaction results with coked catalyst. The catalyst in pretreated by reaction at 450 °C for 10 min with WHSV of 1.5 h^{-1} and then cooled down to 200 °C. The temperature-programmed experiments then start from 200 °C with a temperature rising rate of 50 °C/h. It can be seen that the influence of induction period is also important for coked catalyst. The temperature range of methanol conversion reduction is from 280 to 350 °C, which is longer than that for fresh catalyst. The highest conversion achieved before the induction period is 10%, much lower than that of fresh catalyst (80%). This induction period is critical for operation of MTO pilot-scale setup. Methanol conversion in this temperature range will be very low, and therefore the coke formation is very slow. In the pilot-scale setup, the circulation of catalyst between reactor and regenerator in this temperature range should be avoided.

Figures 23 and 24 depict the methanol conversion and selectivity to light olefins as function of TOS in microscale fluidized bed reactor for different reaction temperature. As can be seen, the lower the reaction temperature, the shorter the duration of the steady state for methanol conversion. Below

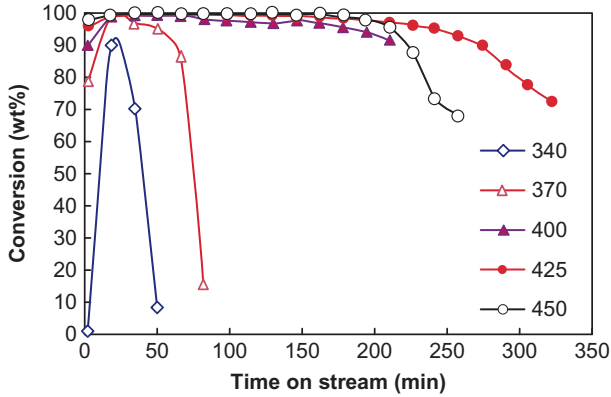

Figure 23 The methanol conversion as function of time in stream for different reaction temperature in the microscale fluidized bed reactor with a WHSV of 1.5 h^{-1}.

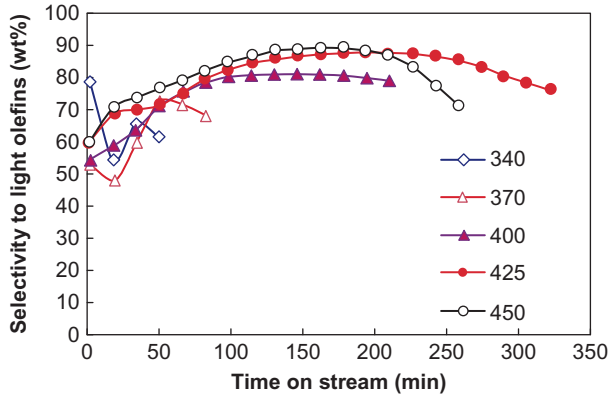

Figure 24 The selectivity to light olefins as function of time on stream for different reaction temperature in the microscale fluidized bed reactor with a WHSV of 1.5 h^{-1}.

370 °C, almost no steady period can be achieved in terms of methanol conversion. This can be explained as the longer induction period at a lower reaction temperature. Actually, the methanol conversion is only 1% at the initial reaction stage under reaction temperature of 340 °C. When the reaction temperature is above 400 °C, the duration of the steady state for methanol conversion increases to 200 min. Such a long steady period is beneficial for the operation in the pilot-scale reactor. Note that the product distribution may change when reaction temperature increases. The selectivity to light olefins (ethylene + propylene) can be maximized above 425 °C.

6.1.5.2 Gas–Solid Contact Time/Space Velocity

The catalyst–gas contact time plays an important part in designing the pilot-scale MTO reactor. Our experimental study confirms that complete methanol conversion can be reached even reducing the reaction contact time to 0.04 s. The contact time has little effect on the conversion is sufficiently high such that the induced period can be avoided. Basically, the shorter the contact time, the higher the selectivity to light olefins. Longer contact time will prompt the side reaction and formation of by-products, which thus decreases the selectivity to light olefins and enhances the coke formation rate. Table 1 lists the methanol conversion and light olefins selectivity for different WHSV. As can be seen, when WHSV increases from 2 to 10 h^{-1}, the MeOH conversion only shows a negligible decline, from 100% to 99.3%. The selectivity to light olefins, on the other hand, increases 81.8–87.5%. This increase is mainly contributed by the ethylene. The selectivity to propylene keeps almost unchanged. Apparently, high WHSV is favorable for reducing the size of industrial reactor while maintaining the methanol feed rate. But in pilot-scale setup, it is generally difficult to design fluidized bed reactor with high WHSV. Table 1 suggests that the results under small WHSV can be extended to large WHSV confidentially. This certainly simplifies the scale-up process of MTO fluidized bed reactor.

6.1.5.3 Side Reactions

In MTO reactor, some side reactions are closely related to the reaction mechanism as well as reaction conditions. As discussed above, the contact time influences the reaction significantly. Ideally, it is expected to control the gas–solid contact time accurately. In laboratory scale microscale fluidized

Table 1 Influence of the Contact Time/Space Velocity: Time on Stream = 5 min, $T = 450$ °C

Contact time (s)	3.05	1.53	1.02	0.76	0.61
WHSV (h^{-1})	2	4	6	8	10
MeOH conversion (%)	100	99.9	99.7	99.6	99.3
Selectivity (wt%)					
C_2H_4	31.2	36.0	37.4	37.3	37.8
C_3H_6	50.6	48.8	49.8	50.1	49.7
$C_2H_4 + C_3H_6$	81.8	84.8	87.2	87.4	87.5

bed reactor, porous filters can be effectively used to separate the catalyst from product gas. In pilot-scale or industrial-scale fluidized bed reactor, the use of filter is not feasible. For example, three stage cyclones have been a common practice for removing the catalyst dust from product gas in FCC processes. Depending on the gas velocity, the entrainment of catalyst to the freeboard can be severe. The amount of catalyst entrained to the freeboard can be much as 20% of the catalyst in the dense bed. Meanwhile, in order to improve the separate efficiency, the gas velocity in the disengaging section can be lower than that in the dense bed. Thus, the side reactions in the freeboard cannot be avoided as the catalyst–gas contact time is prolonged. When scaling up the MTO fluidized bed reactor, it is necessary to realize such difference between the microscale fluidized bed reactor in the laboratory and the large device used in the pilot-scale and/or industrial-scale.

In order to assess the severity of the side reaction, we connect two microscale fluidized bed reactors in series. The first reactor simulates the main MTO reactor and the second simulates the disengaging section in pilot-scale and/or industrial-scale fluidized bed. Methanol is fed to the first reactor, and product gas stream is introduced directly into the distributor of the second reactor. Both reactors are operated at temperature of 450 °C. Catalyst loading in the second reactor is diluted by 33 times the weight of inert particles. The WHSV is the first reactor is 2 h^{-1}. Product gas streams from these two reactors are analyzed with two online GCs. The gas stream from the first reactor is sampled and analyzed every 10 min. The sampling and analysis time of the gas stream from the second reactor is slightly lagging behind. The catalyst loading in the second reactor is ca. 20% of that in the first reactor. Table 2 presents the reaction results. As can be seen, at the beginning of the reaction, the percentages of both ethylene and propylene in the gas product decrease after the product gas passing through the second reactor. The total selectivity to ethylene and propylene drops significantly from 85.83% to 79.74%. Meanwhile, the selectivity to C_4 plus C_5^+ rises from 11% to 17%. This indicates that when the product gas from the first reactor contacts with (relatively) fresh catalyst, the small molecular olefins will convert to high-molecular olefins via polymerization reaction. With the prolonging reaction time (after 10 min), the difference of the selectivity to light olefins between these two product gas streams decreases somehow. Particular interest is the large variation of the selectivity to propylene and C_4 after the second reactor. Clearly, the side reactions will certainly influence the final selectivity to light olefins. In DMTO process, we define our operation window to the regime of high coke content in catalyst, which can prevent the methanol from

Table 2 The Experimental Results for Two Microfluidized Bed Reactors in Series

TOS (min)	2	10	20	30	40	50	60	5	10	20	30	40	50	60
Product Gas (wt%)	**First Reactor: MTO Reaction**							**Second Reactor: Side Reactions**						
CH_4	1.4	1.83	2.24	1.83	1.83	2.11	2.09	1.65	1.95	1.87	1.84	2.03	2.12	2.19
C_2H_4	44.72	41.42	42.91	42.63	42.82	43.91	43.62	42.07	42.67	42.99	43.77	43.87	44.42	44.45
C_2H_6	0.3	0.3	0.48	0.3	0.3	0.33	0.32	0.3	0.33	0.33	0.33	0.33	0.35	0.35
C_3H_6	41.11	41.15	38.58	40.85	41.28	40.61	40.69	37.68	35.63	37.11	38.42	39.08	36.79	36.83
C_3H_8	0.97	1.32	1.85	1.23	1.18	1.18	1.18	1.25	1.53	1.43	1.36	1.25	1.33	1.35
DME	0	0	0	0	0	0	0.16	0	0	0	0	0	0	0
MeOH	0	0	0	0	0	0	0.06	0	0	0	0	0	0	0
C_4	8.89	10.58	10.72	10.26	10.1	9.55	9.55	12.57	13.6	12.73	11.58	10.57	11.73	11.63
C_5^+	2.61	3.4	3.22	2.9	2.49	2.31	2.33	4.48	4.29	3.54	2.7	2.87	3.26	3.2
Total	100	100	100	100	100	100	100	100	100.00	100	100	100	100	100
$C_2^- + C_3^-$	85.83	82.56	81.49	83.49	84.09	84.52	84.5	79.74	78.38	80.1	82.19	82.95	81.2	81.28

complete conversion and maintain a relatively low activity of the catalyst. This can inhibit the side reactions to a certain extent.

6.2 Pilot-Scale MTO Fluidized Bed Reactor

We designed and built a pilot-scale circulating fluidized reactor apparatus, which includes a bubbling fluidized bed reactor and a bubbling fluidized bed regenerator. The overall catalyst loading is 5 kg. The size of the MTO fluidized bed reactor is about 10 cm, and the catalyst inventory is roughly 1 kg. The coke combustion capacity of the regenerator is over-designed in order to ensure the complete regeneration of the catalyst under various operation conditions. Two plug valves are installed to control the circulation rate. Pressure controllers are placed at the product gas outlet of the reactor and the flue gas outlet of the regeneration. The product gas is sampled and analyzed via an online GC. The heat balances has not been considered in our pilot-scale system. Heat required for heating the system and maintaining the reaction and regeneration temperature is supplied by electric heater. Thus, the temperature of the reactor and regenerator can be independently controlled. This is important for flexible operation of the pilot-scale unit.

6.2.1 Fluidized Bed Reaction Without Regeneration

It is necessary to compare the results of the microscale fluidized bed reactor and the pilot-scale fluidized bed. For this purpose, we carried out experiments in the pilot-scale setup under the same operation conditions as in the microscale reactors. Here, the catalyst will not circulate to regenerator. Figures 25 and 26 show the methanol conversion and selectivity to ethylene and propylene, respectively, as a function of TOS in the reactor. Apparently, the results from the pilot-scale reactor as shown in Figs. 25 and 26 fit very well with the results in the microscale fluidized bed reactor (as shown in Fig. 18). A more direct comparison is made for the catalyst-to-methanol ratio shown in Figs. 27 and 28 with Fig. 21, which suggest that the results from microscale reactor and pilot-scale reactor are comparable. Especially, both experiments can reflect the declination of the selectivity to ethylene and propylene with an increasing catalyst-to-methanol ratio. However, the catalyst-to-methanol ratio corresponding to the highest selectivity to ethylene plus propylene is slightly higher in the pilot-scale reactor. This minor difference might be due to the different fluidization behavior in these two reactors. The superficial gas velocity in the microscale fluidized bed reactor is roughly 1/10 of that in the pilot-scale fluidized bed. Thus, the

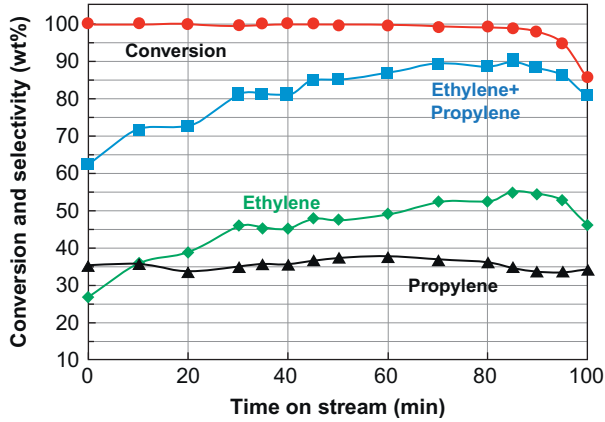

Figure 25 Fluidized bed reaction without regeneration in pilot-scale experiments. Reaction conditions: $T = 460–470$ °C, catalyst inventory = 1 kg, WHSV = 2 h^{-1}, water: MeOH = 20:80, and superficial gas velocity = 25 cm/s.

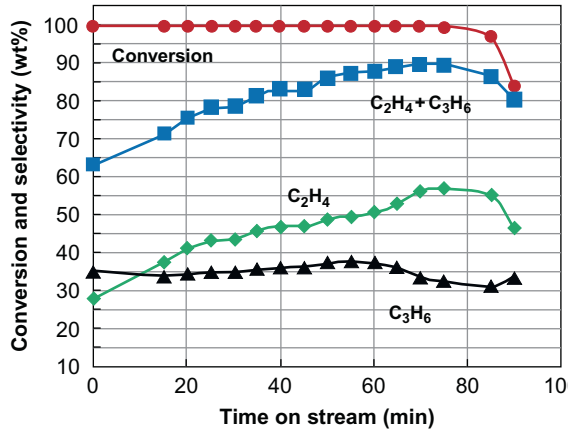

Figure 26 Fluidized bed reaction without regeneration in pilot-scale experiments. Reaction conditions: as the same as in Fig. 25 except $T = 470–480$ °C.

bubble size in the pilot-scale fluidized bed is larger and a worse mass transfer might be expected. Overall, the influence of the hydrodynamics on MTO reaction is not essential, which certainly leads the scaling up of the MTO fluidized bed reactor easier. The agreement between the results from micro-scale fluidized bed reactor and pilot-scale fluidized bed reactor, on the other hand, indicates that the scaling up is successful. The methodologies used in the scaling up indeed provide us right direction.

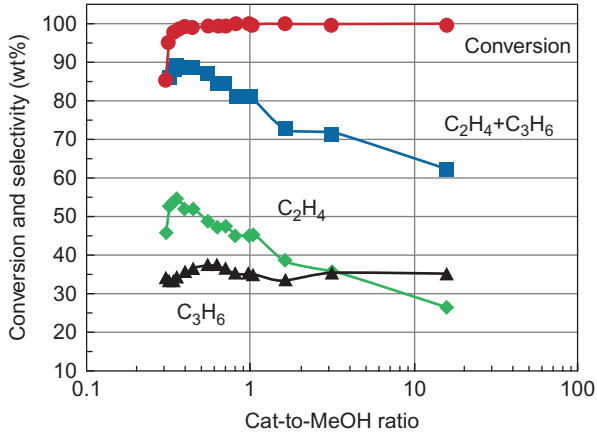

Figure 27 Fluidized bed reaction without regeneration in pilot-scale experiments, as function as catalyst-to-methanol ratio. Reaction conditions: as the same as in Fig. 25.

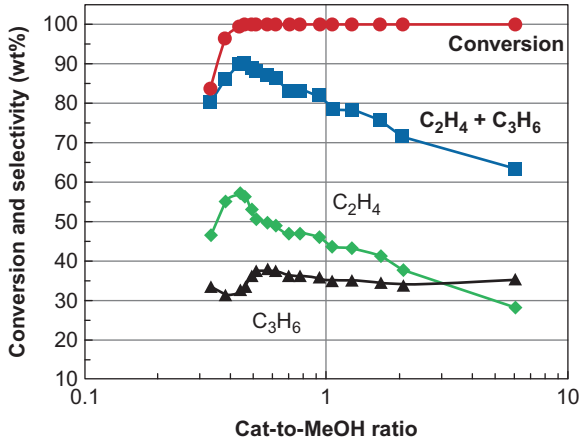

Figure 28 Fluidized bed reaction without regeneration in pilot-scale experiments, as function as catalyst-to-methanol ratio. Reaction conditions: as the same as in Fig. 26.

6.2.2 Fluidized Bed Reaction with Continuous Regeneration

In the pilot-scale experiments, the continuous reaction–regeneration is also investigated. The details of the results will not be discussed here. However, we will focus on the influence of the average residence time and catalyst to methanol on the MTO reaction in pilot-scale fluidized bed reactor.

Figure 29 shows the average residence time of catalyst in the pilot-scale fluidized bed reactor by adjusting the catalyst circulation rate while keeping other conditions such as reaction temperature, inventory, feed rate, and WHSV unchanged. Unlike that in the fluidized bed reactor without catalyst

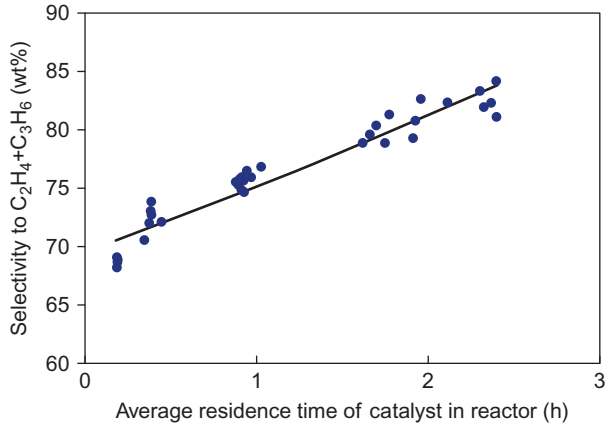

Figure 29 The influence of average residence time of catalyst in reactor on the selectivity of ethylene and propylene. Reaction conditions: $T = 500$ °C, catalyst inventory = 1 kg, WHSV = 2 h^{-1}, water:MeOH = 20:80, and gas–solid contact time = 1.3 s.

circulation, the catalyst circulation will lead to residence time distribution of catalyst in the bed. This means that at any given time, catalyst having different residence time in the reactor may coexist. Some might stay in the reactor for much longer time and meanwhile some might be transported to the reactor just for a short while. Recall that the coke content in catalyst is a function of the residence time as shown in Fig. 19, we can simply assume that a longer residence time of a catalyst might cause higher coke content in it. Note that the optimal coke content is around 7.6–8.5%, it is therefore important to extend the reaction time to prompt the coke content. Therefore, in Fig. 29, the selectivity to light olefins is increased with an increasing average residence time. However, careful check has to be performed to ensure the high conversion of methanol feed.

Figure 30 shows the relationship of the catalyst-to-methanol ratio with the selectivity to light olefins. Compared with Fig. 21, it is interesting to note the qualitative agreement between the pilot-scale results and microscale results. Figure 30 can be used to optimize and control the catalyst circulation rate during the reaction, which on other side suggests that microscale fluidized bed reactor can be effectively used in scaling up the fluidized bed reactor with suitable methodology for analysis.

6.2.3 Continuous Operation of Pilot-Scale Setup

A continuous operation of the pilot-scale MTO fluidized bed reactor has been carried out. Table 3 depicts the mass balance calculation for typical

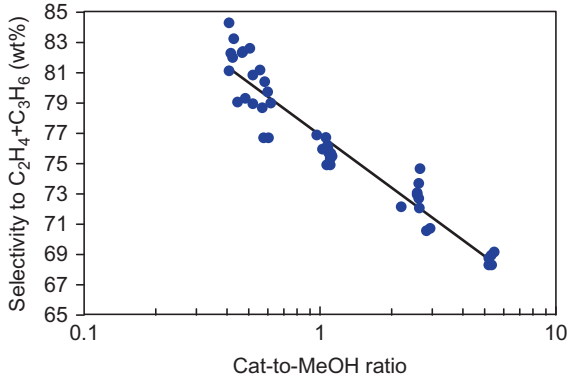

Figure 30 The influence of catalyst-to-methanol ratio in reactor on the selectivity of ethylene and propylene. Reaction conditions: $T = 500\ ^{\circ}C$, catalyst inventory = 1 kg, WHSV = 2 h^{-1}, water:MeOH = 20:80, and gas–solid contact time = 1.3 s.

Table 3 The Typical Mass Balance from Continuous Operation of the Pilot-Scale MTO Fluidized Bed Reactor

Elements			**C**	**H**	**O**
Feed rate (g/h)	CH_3OH	2048.00	768.00	256.00	1024.00
	H_2O	512.00		56.89	455.11
	Sum	2560.00	768	312.89	1479.11
Product gas (g/h)	H_2	0.28		0.28	
	CO	5.00	2.14		2.86
	CO_2	10.00	2.73		7.27
	H_2O	1612.70	0.00	179.19	1433.51
	CH_4	16.40	12.30	4.10	
	C_2H_4	404.71	346.89	57.82	
	C_2H_6	11.14	8.91	2.23	
	C_3H_6	289.12	247.81	41.30	
	C_3H_8	21.84	17.87	3.97	
	CH_3OH	13.90	5.21	1.74	6.95
	Me_2O	3.05	1.59	0.40	1.06
	C_4	89.91	77.07	12.84	
	C_5	34.87	29.89	4.98	
	C_6	8.80	7.54	1.26	
	Coke	20.48	19.25	1.23	
	Sum	2542.20	779.21	311.33	1451.65
Balance		0.99	1.01	1.00	0.98

Reaction conditions: $T = 500\ ^{\circ}C$, Inventory = 1 kg, water:MeOH = 20:40, and WHSV = 2 h^{-1}.
Regeneration condition: $T = 600\ ^{\circ}C$.

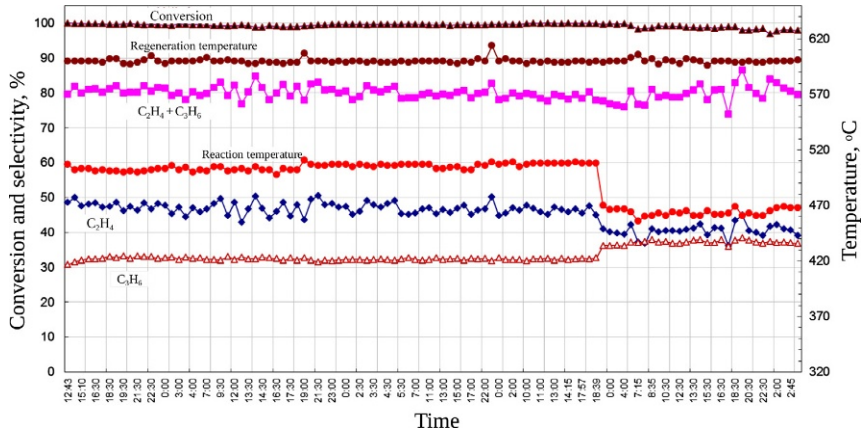

Figure 31 The typical results in the continuous operation of the pilot-scale MTO fluidized bed reactor.

operation conditions. Figure 31 shows the data measured during the operation. As can be seen, methanol conversion is nearly 100% at the reaction temperature of 500–510 °C. The average selectivity to ethylene is 48 wt% and to propylene is 32 wt%. When the reaction temperature is reduce to 460 °C, the average selectivity to ethylene drops to 42 wt% while to propylene increased to 38 wt%. Apparently, the ethylene/propylene ratio can be adjusted by altering reaction temperature. Lower reaction temperature favors propylene production. Based on the mass balance, it is easy to predict that the methanol consumption for producing 1 ton ethylene plus propylene is 2.925 in the continuous operation in the pilot-scale MTO fluidized bed reactor.

7. CHALLENGES AND FUTURE DIRECTIONS

MTO reaction received considerable interests from the viewpoint of either fundamental research or industrial applications. It can be regarded as one of the best examples that can link the work of chemists with chemical engineers. The understanding of the chemistry underlying the methanol conversion over SAPO or ZSM zeolites has been a subject of intense research. The reaction mechanism, i.e., the element reaction steps as well as the intermediate products, is very involved. The reaction itself is not a simple rate-controlling process, and the shape selectivity of the light olefins product can also be related to the molecular diffusion inside the cages and channels of the zeolite crystals. Nevertheless, great advancement has been

achieved in the past decades concerning the MTO reaction mechanism. We expect breakthroughs in the understanding of the first C—C bond formation and reaction path for light olefins generation in the future. From the chemical engineering point of view, there also remain several challenges that need to be addressed in the coming years.

The establishment of mesoscale methods to connect the understanding at molecular (or zeolite crystal scale) to the process controlling at catalyst particle scale (or reactor scale) is highly desired. For example, the mechanism studies seem to support that the hydrocarbon pool mechanism is generally effective for MTO reaction; however, the intermediate carbenium ions vary with the cavity size, and thus, the reaction path may change by altering the crystal structures. Quantitative methods must be developed in order to transfer such understandings into our practice of catalyst design and synthesis. At the reactor scale, the reaction kinetic models are mostly obtained for lumped components via ensemble-averaged experiments. The validity of these models is normally limited to the operation conditions that the experiments have covered. Microscale kinetic models have been researched recently by several groups. A mesoscale approach that can link the microkinetics with the lumped kinetics would be a big challenge.

Another important aspect is how to control coke content distribution in the fluidized bed reactor with catalyst circulation. As we know, there exists optimal coke content for catalyst particle which can maximize the selectivity to light olefins. If there is circulation of catalyst particles, the coke content in catalyst shows a certain distribution. Ideally, if the coke content distribution is uniform such as that encountered in the fluidized bed reactor without circulation, the selectivity to light olefins can reach 90% over SAPO molecular sieves. Therefore, how to optimize the coke content distribution in MTO fluidized bed reactor to improve the selectivity to light olefins represents another future direction.

8. CONCLUSIONS

In this contribution, the process development of MTO process has been introduced. We emphasize the importance of the mesoscale studies in the MTO process development. Particularly, we focus on three aspects: a mesoscale modeling approach for MTO catalyst pellet, coke formation and control in MTO reactor, and scaling up of the microscale-MTO fluidized bed reactor to pilot-scale fluidized bed reactor. The applications of results obtained from these mesoscale studies have been outlined and demonstrated.

As a typical multiphase and multiscale process, the research of MTO process spanning molecules, zeolites, catalyst particles, microscale reactors, and pilot-scale reactors to industrial equipments, cross a wide time and length scales. The development of efficient mesoscale methods are expected for further optimizing the DMTO process and improving fluidized bed reactor design and operation.

ACKNOWLEDGMENTS

The DMTO process development is supported by Chinese Academy of Sciences (CAS), Chinese National Development and Reforming Committee (NDRC), Chinese Ministry of Science and Technology, National Natural Science Foundation of China (NSFC), Government of Shanxi Province, and China Petroleum and Chemical Industry Federation. We are grateful to SINOPEC Luoyang Petrochemical Engineering Co. and SYN Energy Technique Co., and all colleagues involved in the DMTO process development. The authors are supported by the National Natural Science Foundation of China (Grant no. 91334205) and the Strategic Priority Research Program of the Chinese Academy of Sciences (Grant no. XDA07070100).

REFERENCES

Abba IA, Grace JR, Bi HT, Thompson ML: Spanning the flow regimes: generic fluidized-bed reactor model, *AIChE J* 49:1838–1848, 2003.

Alwahabi SM, Froment GF: Single event kinetic modeling of the methanol-to-olefins process on SAPO-34, *Ind Eng Chem Res* 43:5098–5111, 2004a.

Alwahabi SM, Froment GF: Conceptual reactor design for the methanol-to-olefins process on SAPO-34, *Ind Eng Chem Res* 43:5112–5122, 2004b.

Barger P: *Zeolites for cleaner technologies,* London, 2002, Imperial College Press.

Bjorgen M, Svelle S, Joensen F, et al: Conversion of methanol to hydrocarbons over zeolite H-ZSM-5: on the origin of the olefinic species, *J Catal* 249:195–207, 2007.

Bleken F, Bjørgen M, Palumbo L, et al: The effect of acid strength on the conversion of methanol to olefins over acidic microporous catalysts with the CHA topology, *Top Catal* 52:218–228, 2009.

Bleken F, Skistad W, Barbera K, et al: Conversion of methanol over 10-ring zeolites with differing volumes at channel intersections: comparison of TNU-9, IM-5, ZSM-11 and ZSM-5, *Phys Chem Chem Phys* 13:2539–2549, 2011.

Bos ANR, Tromp PJJ, Akse HN: Conversion of methanol to lower olefins. Kinetic modeling, reactor simulation, and selection, *Ind Eng Chem Res* 34:3808–3816, 1995.

Buurmans ILC, Weckhuysen BM: Heterogeneities of individual catalyst particles in space and time as monitored by spectroscopy, *Nat Chem* 4:873–886, 2012.

Campbell CT: Micro- and macro-kinetics: their relationship in heterogeneous catalysis, *Top Catal* 1:353–366, 1994.

Chang CD: A kinetic model for methanol conversion to hydrocarbons, *Chem Eng Sci* 35:619–622, 1980.

Chang CD: Hydrocarbons from methanol, *Catal Rev Sci Eng* 25:1–118, 1983.

Chang CD: Methanol conversion to light olefins, *Catal Rev Sci Eng* 26:323–345, 1984.

Chang CD, Silvestri AJ: The conversion of methanol and other O-compounds to hydrocarbons over zeolite catalysts, *J Catal* 47:249–259, 1977.

Chen NY, Reagan WJ: Evidence of autocatalysis in methanol to hydrocarbon reactions over zeolite catalysts, *J Catal* 59:123–129, 1979.
Chen D, Moljord K, Fuglerud T, Holmen A: The effect of crystal size of SAPO-34 on the selectivity and deactivation of the MTO reaction, *Microporous Mesoporous Mater* 29:191–203, 1999.
Chen D, Grlnvold A, Moljord K, Holmen A: Methanol conversion to light olefins over SAPO-34: reaction network and deactivation kinetics, *Ind Eng Chem Res* 46:4116–4123, 2007.
Chen D, Moljord K, Holmen A: A methanol to olefins review: diffusion, coke formation and deactivation on SAPO type catalysts, *Microporous Mesoporous Mater* 164:239–250, 2012.
Corma A: State of the art and future challenges of zeolites as catalysts, *J Catal* 216:298–312, 2003.
Dahl IM, Kolboe S: On the reaction-mechanism for propene formation in the MTO reaction over SAPO-34, *Catal Lett* 20:329–336, 1993.
Dahl IM, Kolboe S: On the reaction-mechanism for hydrocarbon formation from methanol over SAPO-34 1. Isotopic labeling studies of the co-reaction of ethylene and methanol, *J Catal* 149:458–464, 1994.
Dahl IM, Wendelbo R, Andersen A, Akporiaye D, Mostad H, Fuglerud T: The effect of crystallite size on the activity and selectivity of the reaction of ethanol and 2-propanol over SAPO-34, *Microporous Mesoporous Mater* 29:159–171, 1999a.
Dahl IM, Mostad H, Akporiaye D, Wendelbo R: Structural and chemical influences on the MTO reaction: a comparison of chabazite and SAPO-34 as MTO catalysts, *Microporous Mesoporous Mater* 29:185–190, 1999b.
Froment GF: Coke formation in catalytic processes: kinetics and catalyst deactivation, *Stud Surf Sci Catal* 111:53–68, 1997.
Gayubo AG, Aguayo AT, del Campo AES, Tarrio AM, Bilbao J: Kinetic modeling of methanol transformation into olefins on SAPO-34 catalyst, *Ind Eng Chem Res* 39:292–300, 2000.
Geldart D: Types of gas fluidization, *Powder Technol* 7:285–292, 1973.
Guisnet M: "Coke" molecules trapped in the micropores of zeolites as active species in hydrocarbon transformations, *J Mol Catal A Chem* 182–183:367–382, 2002.
Guisnet M, Costa L, Ribeiro FR: Prevention of zeolite deactivation by coking, *J Mol Catal A Chem* 305:69–83, 2009.
Hansen N, Keil FJ: Multiscale modeling of reaction and diffusion in zeolites: from the molecular level to the reactor, *Soft Matter* 10(1–3):179–201, 2012.
Haw JF: Zeolite acid strength and reaction mechanisms in catalysis, *Phys Chem Chem Phys* 4:5431–5441, 2002.
Haw JF, Song WG, Marcus DM, Nicholas JB: The mechanism of methanol to hydrocarbon catalysis, *Acc Chem Res* 36:317–326, 2003.
Hemelsoet K, Nollet A, Speybroeck VV, Waroquier M: Theoretical simulations elucidate the role of naphthalenic species during methanol conversion within H-SAPO-34, *Chem Eur J* 17:9083–9093, 2011.
Hereijgers BPC, Bleken F, Nilsen MH, et al: Product shape selectivity dominates the methanol-to-olefins (MTO) reaction over H-SAPO-34 catalysts, *J Catal* 264:77–87, 2009.
Hunger M, Seiler M, Buchholz A: In situ MAS NMR spectroscopic investigation of the conversion of methanol to olefins on silicoaluminophosphates SAPO-34 and SAPO-18 under continuous flow conditions, *Catal Lett* 74:61–68, 2001.
Ilia S, Bhan A: Mechanism of the catalytic conversion of methanol to hydrocarbons, *ACS Catal* 3:18–31, 2013.
Jiang R, Wang J, Sun P: Optimization of reactor operating factors a 600,000 TPY MTO plant, *Pet Refin Eng* 44:7–10, 2014 (in Chinese).

Keil FJ: Methanol-to-hydrocarbons: process technology, *Microporous Mesoporous Mater* 29:49–66, 1999.
Keil FJ: Multiscale modeling in computational heterogeneous catalysis, *Top Curr Chem* 307:69–108, 2012.
Knowlton TM, Karri SBR, Issangya A: Scale-up of fluidized-bed hydrodynamics, *Powder Technol* 150:72–77, 2005.
Kortunov P, Vasenkov S, Karger J, et al: Investigations of molecular diffusion in FCC catalysts, *Diffus Fundam* 2:97.1–97.2, 2005.
Krishna R, van Baten JM: Unified Maxwell-Stefan description of binary mixture diffusion in micro- and meso-porous materials, *Chem Eng Sci* 64:3159–3178, 2009.
Krishna R, Wesselingh JA: The Maxwell-Stefan approach to mass transfer, *Chem Eng Sci* 52:861–911, 1997.
Kumar P, Thybaut JW, Svelle S, Olsbye U, Marin GB: Single-event microkinetics for methanol to olefins on H-ZSM-5, *Ind Eng Chem Res* 522:1491–1507, 2013.
Lesthaeghe D, Horre A, Waroquier M, Marin GB, Spey broeck VV: Theoretical insights on methylbenzene side-chain growth in ZSM-5 zeolites for methanol-to-olefin conversion, *Chem Eur J* 15:10803–10808, 2009.
Li J, Ge W, Wang W: *From multiscale modeling to meso-science: a chemical engineering perspective,* Heidelberg, 2013, Springer.
Li H, Ye M, Liu Z: A multi-region model for reaction–diffusion process within a porous catalyst pellet, *Chem Eng Sci* 2015a (submitted).
Li JZ, Wei Y, Chen J, et al: Cavity controls and selectivity: insights of confinement effects on MTO reaction, *ACS Catal* 5:661–665, 2015b.
Liang J, Li H, Zhao S, Guo W, Wang R, Yang M: Characteristics and performance of SAPO-34 catalyst for methanol-to-olefin conversion, *Appl Catal* 64:31–40, 1990.
Liu Z: *Methanol to olefins,* Beijing, 2015, Science Press (in Chinese).
Liu Z, Liu Y, Ye M, Qiao L, Shi L, Ma X: Process technology for DMTO unit with a capacity of 1.8 MM TPY methanol feed and unit features, *Pet Refin Eng* 44:1–6, 2014 (in Chinese).
Matsen JM: Scale-up of fluidized bed processes: principle and practice, *Powder Technol* 88:237–244, 1996.
Mores D, Stavitski E, Kox MHF, Kornatowski J, Olsbye U, Weckhuysen BM: Space- and time-resolved in-situ spectroscopy on the coke formation in molecular sieves: methanol-to-olefin conversion over H-ZSM-5 and H-SAPO-34, *Chem Eur J* 14:11320–11327, 2008.
Mores D, Kornatowski J, Olsbye U, Weckhuysen BM: Coke formation during the methanol-to-olefin conversion: in situ microspectroscopy on individual H-ZSM-5 crystals with different bronsted acidity, *Chem Eur J* 17:2874–2884, 2011.
Nan H, Wen Y, Wu X, Xu C, Guan F, Gong L: Recent development of methanol to olefins technology, *Mod Chem Ind* 34:41–46, 2014.
Olsbye U, Svelle S, Bjorgen M, et al: Conversion of methanol to hydrocarbons: how zeolite cavity and pore size controls product selectivity, *Angew Chem Int Ed* 51:5810–5831, 2012.
Park TY, Froment GF: Kinetic modeling of the methanol to olefins process. 1. Model formulation, *Ind Eng Chem Res* 40:4172–4186, 2001.
Park JW, Lee JY, Kim KS, Hong SB, Seo G: Effects of cage shape and size of 8-membered ring molecular sieves on their deactivation in methanol-to-olefin (MTO) reactions, *Appl Catal A Gen* 339:36–44, 2008.
Primo A, Garcia H: Zeolites as catalysts in oil refining, *Chem Soc Rev* 43:7548–7561, 2014.
Qi L, Wei Y, Xu L, Liu Z: Reaction behaviors and kinetics during induction period of methanol conversion on HZSM-5 zeolite, *ACS Catal* 5:3973–3982, 2015.

Rüdisüli M, Schildhauer TJ, Biollaz SMA, van Ommen JR: Scale-up of bubbling fluidized bed reactors—a review, *Powder Technol* 217:21–38, 2012.
Schoenfelder H, Hinderer J, Werther J, Keil FJ: Methanol to olefins-prediction of the performance of a circulating fluidized-bed reactor on the basis of kinetic experiments in a fixed-bed reactor, *Chem Eng Sci* 49:5377–5390, 1994.
Schulz H: Coking of zeolites during methanol conversion: basic reactions of the MTO-, MTP- and MTG processes, *Catal Today* 154:183–194, 2010.
Song WG, Fu H, Haws JF: Supramolecular origins of product selectivity for methanol-to-olefin catalysis on HSAPO-34, *J Am Chem Soc* 123:4749–4754, 2001.
Song WG, Marcus DM, Fu H, Ehresmann JO, Haw JF: An oft-studied reaction that may never have been: direct catalytic conversion of methanol or dimethyl ether to hydrocarbons on the solid acids HZSM-5 or HSAPO-34, *J Am Chem Soc* 124:3844–3845, 2002.
Stocker M: Methanol-to-hydrocarbons: catalytic materials and their behavior, *Microporous Mesoporous Mater* 29:3–48, 1999.
Sundaresan S: Role of hydrodynamics on chemical reactor performance, *Curr Opin Chem Eng* 2:325–330, 2013.
Svelle S, Ronning PO, Olsbye U, Kolboe S: Kinetic studies of zeolite-catalyzed methylation reactions. Part 2. Co-reaction of [12C]propene or [12C]n-butene and [13C]methanol, *J Catal* 234:385–400, 2005.
Tian P, Wei Y, Ye M, Liu Z: Methanol to olefins (MTO): from fundamentals to commercialization, *ACS Catal* 5:1922–1938, 2015.
Van der Hoef MA, Ye M, van Sint Annaland M, Andrews AT IV, Sundaresan S, Kuipers JAM: Multi-scale modeling of gas-fluidized beds, *Adv Chem Eng* 31:65–149, 2006.
Van Santen RA, van Leeuwen PWNW, Moulijn JA, Averill BA: *Catalysis: an integrated approach,* Amsterdam, 1999, Elsevier.
Van Speybroeck V, van der Mynsbrugge J, Vandichel M, et al: First principle kinetic studies of zeolite-catalyzed methylation reactions, *J Am Chem Soc* 133:888–899, 2011.
Van Speybroeck V, De Wispelaere K, van der Mynsbrugge J, Vandichel M, Hemelsoet K, Waroquier M: First principle chemical kinetics in zeolites: the methanol-to-olefin process as a case study, *Chem Soc Rev* 43:7326–7357, 2014.
Vora BV, Marker TL, Barger PT, Nilsen HR, Kvisle S, Fuglerud T: Economic route for natural gas conversion to ethylene and propylene, *Stud Surf Sci Catal* 107:87–98, 1997.
Wang CM, Wang YD, Liu HX, Xie ZK, Liu ZP: Catalytic activity and selectivity of methylbenzenes in HSAPO-34 catalyst for the methanol-to-olefins conversion from first principles, *J Catal* 271:386–391, 2010.
Wei YX, Li JZ, Yuan CY, et al: Generation of diamondoid hydrocarbons as confined compounds in SAPO-34 catalyst in the conversion of methanol, *Chem Commun* 48:3082–3084, 2012a.
Wei YX, Yuan CY, Li JZ, et al: Coke formation and carbon atom economy of methanol-to-olefins reaction, *ChemSusChem* 5:906–912, 2012b.
Wilson S, Barger P: The characteristics of SAPO-34 which influence the conversion of methanol to light olefins, *Microporous Mesoporous Mater* 29:117–126, 1999.
Wragg DS, O'Brien MG, Bleken FL, Di Michiel M, Olsbye U, Fjellvag H: Watching the methanol-to-olefin process with time- and space-resolved high-energy operando X-ray diffraction, *Angew Chem Int Ed* 51:7956–7959, 2012.
Xu S, Zheng A, Wei Y, et al: Direct observation of cyclic carbenium ions and their role in the catalytic cycle of the methanol-to-olefin reaction over chabazite zeolites, *Angew Chem Int Ed* 52:11564–11568, 2013.
Ying L, Yuan X, Ye M, Cheng Y, Li X, Liu Z: A seven lumped kinetic model for industrial catalyst in DMTO process, *Chem Eng Res Des* 100:179–191, 2015.

Yuan C, Wei Y, Li J, et al: Temperature-programmed methanol conversion and coke deposition on fluidized-bed catalyst of SAPO-34, *Chin J Catal* 33:367–374, 2012.
Yuen LT, Zones SI, Harris TV, Gallegos EJ, Auroux A: Product selectivity in methanol to hydrocarbon conversion for isostructural compositions of AFI and CHA molecular-sieves, *Microporous Mesoporous Mater* 2:105–117, 1994.
Zhang L: Wison engineering successfully commercializes MTO project, *Mod Chem Ind* 33:107, 2013 (in Chinese).
Zhang K, Cheng Y, Li X: Simulation of fluidized bed reactor form methanol to olefins (MTO) process, *J Chem Eng Chin Univ* 26:69–76, 2012.
Zhao Y, Li H, Ye M, Liu Z: 3D numerical simulation of a large scale MTO fluidized bed reactor, *Ind Eng Chem Res* 52:11354–11364, 2013.
Zhu QJ, Kondo JN, Ohnuma R, Kubota Y, Yamaguchi M, Tatsumi T: The study of methanol-to-olefin over proton type aluminosilicate CHA zeolites, *Microporous Mesoporous Mater* 112:153–161, 2008.

This page intentionally left blank